THE TEXAS SURVEY OF RADIO SOURCES COVERING $-35\overset{\circ}{.}5<\delta<71\overset{\circ}{.}5$ at 365 MHz

JAMES N. DOUGLAS, FRANK N. BASH, AND F. ARAKEL BOZYAN[1]
Department of Astronomy, The University of Texas at Austin, Austin, Texas 78712

GEOFFREY W. TORRENCE
Electrical Engineering Research Laboratory, The University of Texas at Austin, Austin, Texas 78712

CHIP WOLFE
Sterling Information Group Inc., P.O. Box 161148, Austin, Texas 78716
Received 1995 November 9; revised 1996 February 14

ABSTRACT

We present the Texas Survey of discrete radio sources between $-35\overset{\circ}{.}5$ and $71\overset{\circ}{.}5$ declination (B1950), which was carried out at 365 MHz with the Texas Interferometer during 1974–1983. The Survey lists accurate positions with internal errors of about an arcsecond, flux densities which for strong point sources have internal errors of about 1% and total errors of about 5%, simple structure models and indications of spectrum and variability for 66841 sources. Results of comparisons with other data are presented, and show that the Survey is 90% complete at 0.4 Jy and 80% complete at 0.25 Jy, is nearly free from spurious sources, and has a lobeshift incidence which is reasonably described by quality flags associated with each source.

1. INTRODUCTION

The University of Texas Radio Astronomy Observatory (UTRAO) has carried out a 365 MHz survey of the sky from $-35\overset{\circ}{.}5$ to $+71\overset{\circ}{.}5$ declination, which was intended to be complete to a flux density level of 250 mJy, to provide positions with an accuracy of about one arcsecond in both coordinates, to give accurate flux densities and indications of source variability, and to give rough structure models for each source.

Observations for the Texas Survey began in early 1974 and were completed in 1983. A preliminary version of one declination strip has been published (Douglas *et al.*, 1980), and a number of intermediate versions of the survey have been privately circulated for various purposes pending completion of the final analysis and adjustment of the data.

The Texas Survey is now complete, and is presented in the following sections. The Texas Interferometer is described in Sec. 2, together with a discussion of the data reduction procedure and the normal and gross errors which may affect catalog entries. Survey observations are described in Sec. 3, with a discussion of the flux and position scales utilized; the Survey catalog of 66841 discrete sources is presented. The completeness, reliability and accuracy (both internal and external) of the Survey are discussed in Sec. 4, and Sec. 5 summarizes the results of the Texas Survey, which is seen to have met all its initial goals, except timely publication!

2. THE TEXAS INTERFEROMETER

The Texas Interferometer is a five-element meridian transit synthesis system which utilizes the space-frequency equivalence of the correlation interferometer for one dimension of directivity and exploits the great ease of multibeaming such devices to provide 120 simultaneous beams. Operating at 335, 365, and 380 MHz, the system attains an rms noise level of about 20 mJy for a completely observed (about 200 nights clustered around four epochs) declination strip.

2.1 Development of the Broad Bandwidth Interferometer

The importance of operating an interferometer at nearly zero total time delay (the ''white light'' fringe) to preserve correlation has been recognized since the beginning of interferometry; the use of a broad bandwidth specifically to provide directivity was first proposed by Vitkevitch (1953), and first used by Goldstein (1959) in solar observations. The multibeam multielement space-frequency synthesis system was proposed in the early 1960's (Douglas 1961; Douglas & Brooks 1962; Douglas 1965). A prototype 245 MHz two-element north-south interferometer with ten simultaneous beams was constructed at UTRAO during 1967 to verify the applicability of these concepts to precise interferometry; accurate declinations of 143 sources were measured and the viability of the technique established (Moseley *et al.* 1970). The exact space-frequency equivalence of a correlation interferometer was theoretically demonstrated by Swenson & Mathur (1969).

Building on this experience, the first five-element version of the Texas Interferometer was constructed during 1968–1970 to demonstrate capability for measurement of accurate coordinates in both right ascension and declination as well as for determination of source structure. This system, which operated at 365 MHz with ten simultaneous beams, was used during 1971 and 1972 to obtain arcsecond positions for about

[1]Present address: 535 Indian Ave., Middletown, RI 02840.

 0004-6256/96/111(5)/1945/19/$6.00

3000 previously cataloged sources (Douglas *et al.* 1973; Ghigo & Owen 1973; Sharp & Bash 1975) together with structure models (Bash *et al.* 1974; Cotton *et al.* 1975).

The final version of the Texas Interferometer came on line in 1974. Enhancements included lengthening two of the array elements for better E-W resolution, increasing the number of simultaneous beams from 10 to 120, equipping the system to operate at 335 and 380 as well as at 365 MHz, and controlling all aspects of data acquisition and calibration with an on-line computer.

Observations for the Texas Survey began in 1974 February (Bash & Douglas 1974; Douglas & Bash 1977); a preliminary version of one declination strip was published in 1980 (7250 sources between 13°5 and 23° declination: Douglas *et al.* 1980). Survey observations were completed in 1983 July. Following six years of further observations to monitor source variability, the Texas Interferometer was shut down in 1989 March.

2.2 *Space-frequency Synthesis*

The design of the Texas Interferometer is based on the space-frequency synthesis technique: two isotropic antennas separated by a baseline of d meters and operated as a correlation interferometer at center frequency f_c with a rectangular bandpass of width $\beta = \alpha f_c$ are equivalent to one isotropic aperture and one linear aperture extended αd meters along the baseline, centered d meters away and operated as a monochromatic interferometer at frequency f_c. The deliberately broadened receiver bandwidth is thus translated into a significantly widened spatial-frequency response.

The width in angle space of the envelope beam of this equivalent interferometer is $\lambda/\alpha d$ radians, with pointing determined by the precorrelation time delay. Many beams at different angles to the interferometer baseline may be obtained simultaneously by the economical expedient of operating many correlators at various time delays. An entire group of simultaneous beams may be steered by a single variable delay line, and the amount by which the steering has been changed is readily and accurately determined by observing the phase of two stable monochromatic signals fed through the delay system.

A number of such interferometers may be arranged so that the extended apertures equivalent to each just touch, thereby synthesizing a larger linear aperture while retaining the great ease of steering and multibeaming.

The directivity obtained by space-frequency synthesis is in the direction of the interferometer baseline; the other dimension of directivity must be obtained by using linear arrays perpendicular to the baseline instead of isotropic elements, or by using earth rotation synthesis in addition to space-frequency synthesis. The required sensitivity per unit time is obtained by suitable choice of antenna effective area, taking into account the relatively high sensitivity per unit area produced by the large bandwidth of the system.

The large bandwidth also heightens the vulnerability of the system to interference, but in a sporadic interference environment this is more than offset by the greatly increased information rate from multiple simultaneous beams. Multiple beams also make the job of detecting and rejecting interference easy: interference is quasi-monochromatic and therefore appears with equal amplitude in all beams, while sources have a broad spectrum and appear in only a few. The response of the system does depend on the (unknown) spectral index of the source, but only to second order, and even that dependence vanishes when the source is observed at zero total time delay, i.e., in the peak of the envelope pattern.

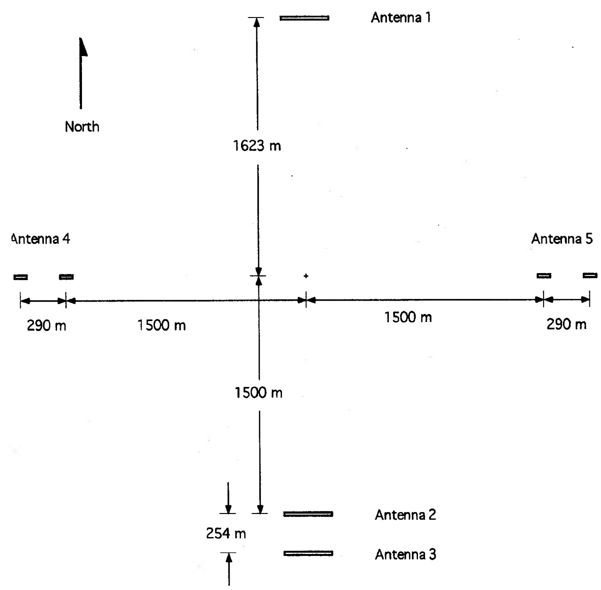

FIG. 1. Layout of the Texas Interferometer. Antennas 1, 2, and 3 are 300 m, E-W linear arrays of 128 helices each. Antennas 4 and 5 are each summing interferometers composed of two 75 m, E-W linear arrays of 32 helices each.

2.3 *Arrangement of the Interferometer Elements*

The Texas Interferometer as used in the Survey consists of five antennas located near the vertices of a three-by-three km diamond as shown in Fig. 1. All five antennas are east-west linear arrays of identical right-circular bifilar helix antennas.

The bifilar helix element is 9.875 in. in diameter, 170.625 in. long, and has 20 turns with a pitch angle of 15°4. This particular design was chosen to provide a good beam pattern and impedance match over the frequency range 300–450 MHz. A single helix element at 380 MHz, the highest frequency used in the Survey, has a measured beam width of 22°1 (full width to half maximum) and a beamwidth to first nulls of 42°8; the half-power beamwidth is proportional to λ^2; the beamwidth to first nulls is proportional to $\lambda^{1.8}$. The beamwidths at 335 MHz, the lowest Survey frequency, are 28°6 to half power and 52°3 to first nulls.

Antennas 1, 2, and 3 are east-west line arrays of 128 helix elements each. The helices are uniformly spaced on 7.5 foot centers, so the outermost elements are separated by 952.5 feet. Antennas 4 and 5 are summing interferometers, each composed of two 32-element east-west line arrays with uniform 7.5 foot element spacing. The subarray centers are spaced by 952.5 feet east-west, i.e., by a distance identical to the length of antennas 1, 2, and 3.

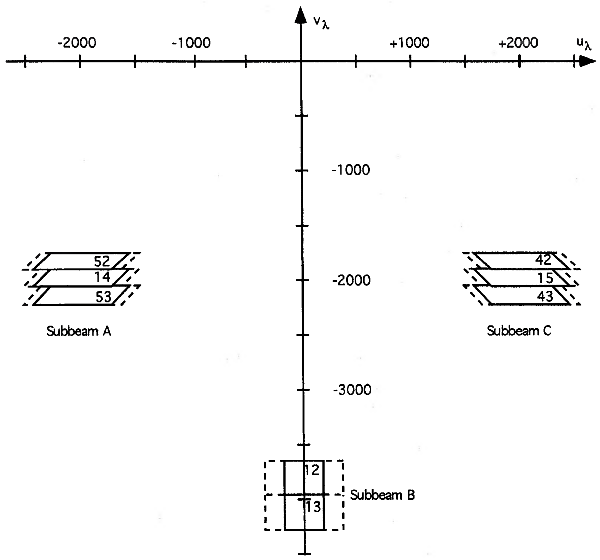

FIG. 2. Spatial frequency response at the zenith of the Texas Interferometer at 365 MHz. Dotted lines enclose regions of nonzero response; solid lines outline the equivalent width.

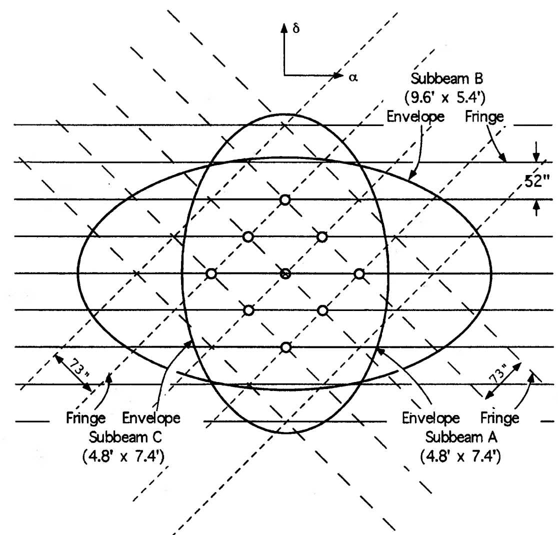

FIG. 3. Angle space response at the zenith of the subbeams of the Texas Interferometer. Solid lines outline the half-power points of the envelope of the subbeams, and circles designate the diamond grid of most probable lobeshift positions. Note that the celestial sphere is viewed from outside, right ascension increasing to the right.

Eight of the ten interferometer pairs possible with these five antennas are used in the survey; their spatial frequency response at the center frequency of 365 MHz is shown in Fig. 2.

Note that the broad operating bandwidth (30 MHz, or about 8% of the center frequency) results in spreading the spatial frequency response of each baseline, in the direction along the baseline, from the east-west lines characteristic of monochromatic operation (corresponding to a fan beam in angle space) into rectangles or parallelograms of substantial size (corresponding to an envelope beam narrow in both coordinates). Thus, for example, operation of antennas 1 and 2 together produces baseline 12, whose spatial frequency equivalent width is 356 wavelengths in u (produced by the east-west length of the line arrays) and is 337 $\cos z$ wavelengths in v (produced by the broad bandwidth; z is the zenith distance). The corresponding envelope beamwidth in angle space for baseline 12 is 9′.6 east-west by 10′.2 $\sec z$ north-south.

The relative placement of antennas has been chosen so that the spatial frequency response of the eight baselines used falls into three patches of contiguous sensitivity, which we call *subbeams*. Subbeam A comprises baselines 52, 14, and 53, subbeam B comprises baselines 12 and 13, and subbeam C comprises baselines 42, 15, and 43. These approximately rectangular patches (713 wavelengths $\times 462 \cos z$ wavelengths for A and C, 356 wavelengths $\times 634 \cos z$ wavelengths for B) produce compact envelope subbeams in angle space (4′.8 by 7′.4 for A and C, 9′.6 by 5′.4 for B, at the zenith). Subbeam A is a 2800 wavelength interferometer in azimuth 225° (73″ fringe spacing), subbeam B is a 4000 wavelength interferometer in azimuth 180° (52″ fringe spacing), and subbeam C is a 2800 wavelength interferometer in azimuth 135° (73″ fringe spacing). The envelope and fringes are shown in Fig. 3.

The grouping of the spatial frequency samples in the three subbeam patches (see Fig. 2) produces a sparse and regular sampling of the u-v plane. Such sparse sampling means that the angle-space description of sources observed is model dependent. Even flux density and centroid position, which are directly (if possibly inaccurately) observable with a pencil beam instrument, with our instrument depend on the model adopted.

Furthermore, the system has zero response to any spatial frequencies below about 2500 cycles per radian and sufficiently large source components will be attenuated to undetectability. For example, a circular Gaussian source with full width to half maximum of 66 arcsec will have a fringe visibility of less than 0.1 on all baselines; a 94 arcsec Gaussian source will have a fringe visibility less than 0.01. Thus, continuum radiation from the galaxy, and indeed most galactic sources, will be fully resolved and hence invisible.

On the other hand, Gaussian sources or individual source components with full width to half maximum less than 8 arcsec will have fringe visibility greater than 0.9 on all baselines. The net fringe visibility on a given baseline of a large double with compact components of course will depend on its orientation and spacing.

The concentration of spatial frequency samples into three subbeam patches in the u-v plane of different orientation and length means that while sufficiently strong doubles with compact components will be listed regardless of their separation or orientation, the limiting flux density of the Survey will in fact be somewhat dependent on the double's orientation and spacing. For example, a 26 arcsec north-south double will be at a fringe null for subbeam B, although fully visible in subbeams A and C. If point sources with flux densities greater than 0.25 Jy are detected in the Survey with a certain reliability, a universe filled with doubles of this type would be surveyed to comparable reliability to a flux density of 0.5 Jy. This factor of 2 is the worst case (matched by the case of oblique doubles which are simultaneously near zero fringe visibility in subbeams A and C but near full visibility in subbeam B).

This same concentration also gives rise to the possibility of more than one double model fitting noisy data (''structure lobeshifts''—see Sec. *2.6.2* below).

The effect of our joint treatment of the three subbeams is that two sources of comparable strength will be separately listed in the catalog if separated by more than 9$.^s$ sec δ in right ascension or by more than 7$'$.4 sec(δ−30°) in declination, or will be successfully modeled as a double source if separated by more than 20$''$ but less than 2$'$. Double sources separated by less than 10$''$ are unresolved by the system, appearing as point sources, while those with separations between 2$'$ and 10$'$ are poorly modeled and usually flagged as such.

The coadded angle-space pattern of all eight baselines is quite complex, and is never directly used. It is useful, however, in considering the overall possible effect of confusion. The total equivalent u-v area of the eight baselines in the lower half of the u-v plane is 884 700 square wavelengths. If one combined all eight baselines with equal weight to produce a synthesized beam in angle space, the equivalent antenna envelope solid angle would be 12.7 square arcmin. This corresponds to 283 envelope beams per square degree, or 884 700 beams per steradian, which is adequate for accurate work at the Survey surface density of about 7000 sources per steradian.

2.4 Observing Cycles

Instantaneous meridian coverage of a declination strip about 9° sec z wide is achieved by operating 120 complex correlators at different time delays (for the north-south baselines) or 60 correlators (for the oblique baselines, whose declination beam spacing is twice that of the north-south baselines). The single 120-beam backend can handle either one north-south or two oblique baselines. Thus five days' observing (configuration 12: baseline 12; configuration 13: baseline 13; configuration 145: baselines 14 and 15; configuration 245: baselines 42 and 52, and configuration 345: baselines 43 and 53) are required to record the instrument response of all 8 baselines to the total solid angle of a declination strip (about 3200 cos δ sec z square degrees).

This five day sequence produces data on all 8 baselines with a synthesized rms noise of about 100 mJy per baseline; 8–12 such five day sequences are obtained in a contiguous 40–60 day observing *cycle*. Following a computer scan for interference and equipment malfunction, several hundred strong sources are used to reduce the amplitude and phase system of each night to that of a mean night, which in turn is calibrated to first order by using several dozen sources of known position and flux density. The nightly data from each baseline are then corrected and averaged over the cycle. The cycle mean data for each of the eight baselines are the fundamental output of the system which is used in further analysis: the noise level is low enough (about 40 mJy per baseline) for survey purposes; interference has been removed; ionospheric fluctuations have been smoothed and systematic gain and phase variations removed. Gaps produced by interference or by equipment malfunction appear only as variable redundancy in the data.

Initial survey plans involved using only night-time observations, thereby requiring three observing cycles to obtain a complete set of cycle mean data. Early experience with the data showed that daytime observations were also usable, the regular diurnal refraction component being removable except for brief periods near sunrise and sunset. Unfortunately, the same experience also showed that to attain full accuracy and reliability for sources as weak as 250 mJy four observing cycles split between two center frequencies would be required. The use of four cycles improves sensitivity and accuracy, and provides an opportunity to study source flux density variability, while the use of two frequencies significantly reduces lobeshift incidence and also expands the u-v plane coverage by about 50%. The redundancies in observation epoch and in frequency are both of great assistance in the reliable distinction of real sources from spurious responses. This alteration in observing strategy explains why only the first two cycles observed (at +18° and +36°) were at the survey nominal center frequency of 365 MHz. Subsequent cycles of these strips, and all cycles of other strips, were split between operating frequencies of 335 and 380 MHz.

2.5 Analysis Procedure

The basic telescope output may be considered to be the cycle-mean complex fringe amplitudes $z_{kc}(\alpha_j,\delta_i)$ for the eight baselines k=1,8 on each of the four observing cycles c=1, 4 or 32 complex numbers for each direction α_j,δ_i in an oversampled grid of directions comprising a declination strip. Each z_{kc} is an estimate of the spatial frequency spectrum averaged over a rectangle centered on u_{kc},v_{kc} cycles per radian. One observing cycle provides eight separate and nonoverlapping u-v samples (see Fig. 2). The use of four observing cycles at two frequencies provides redundancy and gives additional u-v samples, but also require the inclusion of the spectrum of the source and its (possibly variable) flux density at four epochs as unknowns.

The initial process of analysis of a declination strip proceeds in two stages: First, we locate sources in the strip, producing a catalog of candidates (''enumeration''), and second, we analyze the 32 z_{kc} values at the position of each candidate source to verify its existence and to estimate its parameters according to some adopted model, the model itself being deduced from the data (''characterization'').

2.5.1 Enumeration

Subbeam fringe amplitude maps for each subbeam s and cycle c are prepared by converting the two or three z_{kc} values within each to a synthesized cycle subbeam response z_{sc} for each grid point α_j,δ_i; the magnitude of this response R_{sc} is written on tape for further processing. We thus have available twelve (s=A,B,C; c=1,4) independent fringe amplitude maps of the strip, which for compact sources are equivalent to 4'.8 by 7'.4 (A,C) or 9'.6 by 5'.4 (B) pencil beam scans of the strip.

The cataloging program (FINDER) operates separately on each of these 12 cycle subbeam maps. Sources are located and treated in descending order of flux density, the effect of stronger sources being subtracted from the map before proceeding to the next weaker one. Position, peak flux density and beam-weighted flux density are listed for each source. This process is iterated until flux densities fall below 170 mJy (the rms noise on a cycle subbeam map is 50–75 mJy). In this manner 12 independent catalogs of the strip are produced for four epochs, on at least two frequencies (and thus two different sidelobe structures) and for three mean baselines, again with different beam shapes and sidelobe structures. Although not as independent as if produced by 12 different observatories, the catalogs are completely independent as regards noise and time-dependent instrument problems, and significantly independent as regards confusion and sidelobe contributions.

A merged catalog is then produced for further analysis. To be included a source must appear in six or more subcatalogs, or in all four subcatalogs of the same subbeam (thereby including double sources with certain orientations which would have otherwise been missed) or in all three subbeams of a given cycle (thus including variable objects such as Cyg X-3, whose flux density may be above the catalog limit in only one cycle). Few spurious responses will survive this process, and few real ones will be excluded. The criteria have been set, however, to minimize the chance of a real source being lost, since spurious sources may be readily detected and removed at later analysis stages, while an excluded real source is lost forever, at least to this analysis.

2.5.2 *Characterization*

The merged catalog forms the input to the main analysis program SYNAPSE. The 32 complex numbers at the position of each source (and their covariance matrix) are gathered together, and further calibrations are applied both to the z_{kc} and to the covariance matrix to place all four cycles on the same (but not necessarily final) position and flux scale. A hierarchy of models of ascending numbers of parameters is fitted to the data by an iterative non-linear least-squares procedure. The simplest acceptable model is chosen, or the least unacceptable one is adopted, in which case the source is flagged as poorly modeled.

The simplest model (point source or P) involves six parameters: source position (α,δ) and flux density on each of the four cycles (S_1,S_2,S_3,S_4). This is a total of 6 real numbers from data totaling 64 (partly correlated) real numbers. The two more complicated models are both double models with gaussian components of full width to half maximum equal to 19% of their spacing. The symmetric double (D) assumes the components have equal flux density, and two further parameters are added: the separation of the components r and position angle χ—a total of eight parameters. The asymmetric double (AD) is assumed to have different component flux densities $S_a > S_b$; a further (asymmetry) parameter q is required and is defined as $q=(S_a-S_b)/(S_a+S_b)$. Note that an AD with $q=0$ is the same as a D model; an AD with $q=1$ would be a P model.

More elaborate models are possible without exhausting the number of degrees of freedom of the system. The most obvious such extension would be to solve for the component sizes, but Monte Carlo experiments showed that these would be poorly determined due to the lack of data at low spatial frequencies and the concentration of samples near two values of u^2+v^2. Fortunately, at our resolution, radio sources mostly do look like either point or double structures. We can retain the substantial degree of overdetermination which permits internal estimates of error and assessments of the suitability of the model chosen.

Values of the parameters for the model chosen and their covariance matrix constitute the characterization of the source. Following SYNAPSE a program (RAPTURE) calculates flags (indicating quality of model fit, the source environment, and lobeshift likelihood), fits a mean flux density and spectral index to the cycle fluxes, and calculates squared standardized residuals to this fit which can indicate possible source variability (as can a strange spectral index) and applies the penultimate flux and position scale adjustments.

2.5.3 *Removing spurious sources*

The merged catalog which was scanned by SYNAPSE and RAPTURE contained many spurious sources, most of which were detected (e.g., by noting near zero or negative flux, or by very low signal-to-noise ratio) and removed by these analysis programs. However, a number of spurious sources remain following RAPTURE. A filter algorithm which utilizes the RAPTURE flags, the source flux and signal-to-noise ratio, and the source structure was devised by trial and error which removed the vast majority of the remaining spurious sources at the expense of losing only a few real ones. This algorithm was adjusted by comparisons with other radio surveys and in particular a set of Arecibo 21 cm observations on the +18° strip (Douglas & Davis 1981). This filter algorithm was then applied to each strip catalog, without special treatment being given to the few sources the algorithm was known to treat wrongly. Thus a few real sources are known to be in our discard list, and a few sources we know to be spurious remain in the catalog.

2.6 *Errors*

Errors quoted in the catalog are internal, based on the observed residuals to the least squares adjustment, or on the propagated error from individual nightly observations, whichever is larger. Parameters in a source listing may be off by substantially more than the stated error, however, due to *position lobeshifts, structure lobeshifts, or poor models.*

2.6.1 *Position lobeshifts*

All measurements made interferometrically on the meridian are susceptible to position lobeshifts. Lobe selection is carried out by SYNAPSE based on three kinds of internal information: the envelope source position as determined in the 12 FINDER catalogs, the residuals to the chosen model (which are higher at an incorrect lobe position) and the flux density in subbeams for the chosen model (which is lower at an incorrect lobe position). SYNAPSE inspects the quality of contrast between the chosen and the second most likely lobe positions; if the decision is difficult the source is flagged as possibly lobeshifted. In such cases, if the second most likely position is clearly better than the remaining ones, its offset is listed in the catalog; otherwise no attempt is made to predict the direction of a possible lobeshift. A lobeshifted source will have in addition to its gross position error some additional error in its flux density and model parameters.

2.6.2 Structure lobeshifts

Due to the regular spacing of the three subbeam patches in the u-v plane more than one double model can be consistent with a set of complex subbeam fringe amplitudes, although only the correct double model will accurately reflect the small changes in fringe visibility on the various baselines within a subbeam. For noisy or confused data the incorrect model may sometimes be chosen.

For example, consider a source at 30° declination which is double, separated by 73 arcsec in position angle 45°. This source is extended in a direction perpendicular to the subbeam C baselines and is seen by them as unresolved, while its fringe visibility is at the negative peak beyond the first null on both subbeam A (fringe spacing 73 arcsec, double extended along the subbeam A baseline) and subbeam B (fringe spacing of 52 arcsec, which is the north-south component of the double's separation). This source has equal amplitude in all three subbeams, just like a point source, and the 180° phase shift in subbeams A and B can be removed by shifting the listed position of the source by half a lobe in each coordinate. If the small differences between the baselines within the subbeams are obscured by noise or distorted by confusion, this large double might appear in the catalog as a point source with a significantly underestimated flux density and a position offset of one-half lobe in each coordinate. We call this problem a *structure lobeshift.*

The structure lobeshift phenomenon is not restricted to sources which appear point-like, but is more general, and is illustrated in Fig. 4. A source which is actually a 32 arcsec double in position angle −72° (arrow "1") might be listed instead as a 66 arcsec double in position angle 20° (arrow "3") with its position offset by 26 arcsec in each coordinate and a substantially overestimated flux density; or if the source had the larger structure, it might be listed with the smaller. Arrows "2" and "4" are also possible structure lobeshifts, as are numerous others not shown. In cases of doubt, the program adopts the smaller or simpler model.

2.6.3 Lobeshift algorithms

Alternative position lobe coordinates and structure lobe separations and position angles cannot be calculated exactly without reanalysis, since weighted means of many baselines are involved. However, an approximate algorithm may be used, which is based on regarding subbeams A, B, and C as monochromatic isotropic interferometers whose southern elements are in azimuths 225°, 180°, and 135°, respectively, with spacing of $4000/\sqrt{2}$ wavelengths for A and C and 4000 wavelengths for B. Thus, subbeams A, B, and C sample

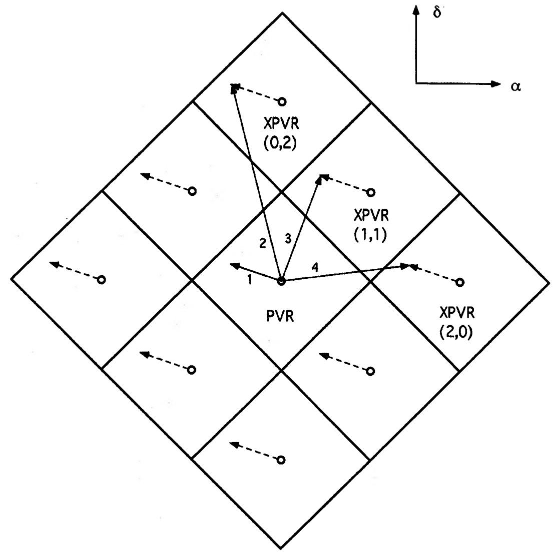

FIG. 4. Tiling of structure space for asymmetric double models. The principle value region (PVR) is at the center, and the arrow designated "1" shows the separation and orientation of a double model of $\beta_x = -30''$, $\beta_y = +10''$($R = 32''$, $\chi = -72°$). Surrounding diamonds are "XPVR" regions, and double models offset from their centers by the same amount as the PVR model are alternative structure models. Three are shown here: the arrow designated "2" has $k_x = 0$, $k_y = 2$ and thus $\beta'_x = 30''$, $\beta'_y = +10'' + 2 \times 52'' = 114''$, or $R = 118''$ and $\chi = -15°$. The arrow designated "3" is the (1,1) structure lobeshift: $R = 66''$, $\chi = 20°$; the arrow designated "4" is the (2,0) structure lobeshift: $R = 75''$, $\chi = 82°$.

(u,v) coordinates (−2000, −2000), (0, −4000), and (2000, −2000) cycles per radian, respectively. This regular sampling leads to a tiling of structure space with diamond-shaped regions, as shown in Fig. 4. The stronger component of the double is taken to be at the center of this diagram, and the structure is described by the arrow pointing to the location of the weaker component. The diagonal lines are the fringe visibility nulls on baselines A and C, and are spaced by about 73 arcsec. The three subbeam amplitudes and three subbeam phases for a source permit determination of flux, asymmetry parameter, separation, position angle, right ascension, and declination of the source—six parameters from six observations. The central diamond, or principal value region (PVR), contains double models whose fringe visibility is inside the first null on subbeams A and C; one such model is produced by data from every source. Every source also has solutions in each of the other diamonds as well; the location of the point representing the solution is in the same position relative to the center of the offset diamond as the PVR solution is with respect to the center of the diagram.

Suppose the catalog position is α, δ and the listed double model has separation R arcsec in position angle χ, corresponding to cartesian component separation $\beta_x = R \sin\chi$ in $\alpha\cos\delta$ and $\beta_y = R\cos\chi$ in δ.

Then, alternative structure lobe components β'_x, β'_y are given by

$$\beta'_x = \beta_x + k_x \lambda_x ,$$

$$\beta'_y = \beta_y + k_y \lambda_y ,$$

TABLE 1. Observed declination strips.

Observation Strip	Declination Limit Lower	Declination Limit Upper	Cycle Epochs 1	Cycle Epochs 2	Cycle Epochs 3	Cycle Epochs 4	Ω (sr)	#
−26°	−35 46 50	−18 14 18	1975.30[c]	1977.15[a]	1979.40[a]	1981.08[c]	1.707	9398
−12°	−19 04 38	−6 04 31	1975.44[c]	1977.91[a]	1979.22[a]	1981.25[c]	1.389	8480
−01°	−6 51 36	4 19 03	1975.94[c]	1976.42[c]	1977.40[a]	1980.20[a]	1.224	8045
+09°	3 34 18	14 00 59	1975.77[c]	1978.08[a]	1979.05[a]	1981.43[c]	1.130	7770
+18°	13 11 33	23 01 26	1974.21[b]	1974.99[c]	1975.60[c]	1976.82[a]	1.023	7499
+27°	22 18 32	32 02 34	1977.49[a]	1979.62[a]	1980.88[c]	1982.95[c]	.948	6244
+36°	31 28 52	40 59 02	1974.32[b]	1974.81[c]	1975.15[c]	1976.98[a]	.840	6430
+45°	40 21 37	50 23 28	1976.10[c]	1977.73[a]	1980.02[a]	1983.42[c]	.772	5055
+55°	49 40 46	60 11 30	1976.24[c]	1978.25[a]	1979.81[a]	1982.73[c]	.661	4522
+65°	59 44 12	71 35 00	1976.36[c]	1978.43[a]	1978.58[a]	1983.23[c]	.534	3398

[a]335 MHz
[b]365 MHz
[c]380 MHz

where k_x and k_y are integers whose sum k_x+k_y is even, and where, for the $+18°$ and $+36°$ strips, we have

$\lambda_x = 51.45$ arcsec, the lobe interval in $\alpha \cos \delta$,

$\lambda_y = 52.02 \sec z$ arcsec, the lobe interval in δ,

and for the other strips, due to a different combination of observing frequencies,

$\lambda_x = 52.57$ arcsec,

$\lambda_y = 53.15 \sec z$ arcsec,

where z is the zenith distance of the source at the effective latitude of the subbeam B interferometer: 30° 00′ 33″ north.

For structure lobe (k_x, k_y), the alternative position lobes α', δ' are

$$\alpha' \cos \delta' = \alpha \cos \delta + \left(k_\alpha + \frac{k_x(1-q)}{2} \right) \lambda_x,$$

$$\delta' = \delta + \left(k_\delta + \frac{k_y(1-q)}{2} \right) \lambda_y,$$

where k_α, k_δ are integers whose sum $k_\alpha + k_\delta$ is even.

2.6.4 *Poorly modeled sources*

Not all sources are well modeled even by the asymmetric double model; if such a source is relatively strong, there will be a noticeable enhancement of the residuals to the best-fitting model. The best-fitting model is then listed, but the inadequacy of the model is characterized by a flag. In such cases, the listed parameters may be approximate or even accurate guides to position, strength and scale of the source; on the other hand they may be substantially in error or totally misleading. The probability of such difficulties is greatest for sources with angular scale between 2′ and 10′, or component sizes of 30″ or more, and inevitably some such sources when sufficiently faint will not be flagged as poorly modeled.

3. THE TEXAS SURVEY

3.1 *The Observations: Cycles and Strips*

Survey observations were carried out in ten overlapping declination strips. Each strip was surveyed for four observing cycles, at two or three frequencies. These observation declination strips are listed in Table 1, together with the extrema of declination in 1950 coordinates, the epoch and frequency of each observing cycle, the solid angle, and the number of sources for each strip.

The overlapping coverage (about 40′–50′) produces independent observations of sources on the boundaries of strips, and after reduction, independent catalog lines. This affords an opportunity to check the position and flux scales of adjacent strips; the listing with the better signal-to-noise ratio and/or model fit is retained for the Survey. The numbers in Table 1 reflect counts after removal of these duplicate listings.

3.2 *Reduction to Sky*

Each observing cycle of each strip is independently calibrated to first order by the use of 320 strong sources to refer the amplitude and phase scales of the nights of the cycle to a common mean night, and by the use of 20–40 point sources whose positions and flux densities are adopted as standards to refer the mean night to the sky. The primary goal of this calibration is to insure that there are minimal variations in the phase/amplitude systems among baselines on a cycle, so that synthesized beams are as undistorted as possible—vital considerations in the choice of structure models and selecting position and structure lobes. The process produces a reasonably good position and flux scale as well, and no further calibration is done until a preliminary version of the final survey catalog is complete, when a final reduction to sky is undertaken.

At the time of final reduction to sky, we are dealing with synthesized data rather than nightly data, and thus can use much weaker calibrators. Furthermore, structure models are sufficiently successful to permit the use of flux density calibrators which are not point sources—a particularly important point, since point sources of known flux density are rare, and are apt to be variable as well. The final reduction to sky only provides corrections to the position and flux systems of the declination strips–no adjustments to individual cycles or baselines are made, so structure and variability and lobeshift choices are unaffected. However, small right ascension- or declination-dependent adjustments in the flux and positions can be made, to remove the small residual systematic errors in the mean night due, for example, to uncompensated ionospheric refraction or diurnal gain changes. For this purpose, a large set of calibrators is desirable.

3.2.1 *Position*

The accuracy of the best radio astrometric positions is unsurpassed at any wavelength; positions of hundreds of compact sources are available to milliarcsecond precision. However, the compact objects to which these cm-wavelength measurements refer may be surrounded by steep spectrum distributed emission, so that in practice the 5 GHz position may deviate from the 365 MHz position for some objects by an arcsecond or more—while for other objects, compact at both frequencies, the deviation may be zero. Lacking 365 MHz structure information on the arcsecond level for most potential calibrators, we cannot restrict our attention to those calibrators with no frequency dependence of centroid position, and thus must use a large number of calibrators of less than ultimate accuracy. A large number would be necessary in any case for eliminating systematic effects in the position system.

A set of 2281 position calibrators over the entire sky was compiled from the literature, which included radio sources with interferometrically determined positions with standard deviations of 2 arcsec or better in both coordinates. The survey area contained 2127 of these sources, and 1852 of these actually appear in the Survey, the missing ones being typically relatively faint sources with flat spectra which are below the Survey flux limit. The 1852 position calibrator sources actually found in the survey include a number which are not suitable for calibration purposes: 27 have noise-to-signal ratio greater than 0.15; 204 are asymmetric double sources with q greater than 0.15 and thus likely to have centroid offsets; 109 have poor models or are affected by near-by sources; 74 have lobeshifts or structure lobeshifts, and 96 have combined survey-calibrator position errors greater than 2 arcsec in either right ascension or declination—a total of 510 sources rejected for cause. The remaining 1342 sources were used in the final adjustment of the position system of each declination strip, but of this number 308 were removed in the course of adjustment for excessive deviation, leaving a subset of 1034 position calibrator sources which determine the Texas Survey position system.

3.2.2 Flux density

The Survey flux scale is defined by the adopted 365 MHz flux density of 582 flux calibrators: sources not initially known to be time variable at meter wavelengths, and whose Survey catalog entries have the correct position and structure model.

Meter-wavelength flux densities are based on scales established in the 1960's and 1970's and remain much more poorly known than cm-wave flux densities. Individual source flux densities have errors of 5% or more, and more seriously, the flux scales themselves are probably affected by significant systematic error both as a function of source flux density (see, e.g., Scott & Shakeshaft 1971), and as a result of the possible incorrect adjustment for the secular decrease in the flux density of Cas A (Rees 1990).

The basis for the Texas Survey flux densities is a slightly modified version of the flux scale developed by Wills (1973; herein referred to as the ''BW scale''). The BW scale was recreated from basic flux data, rereduced and modified to reflect an assumed frequency-independent secular decrease of the flux density of Cas A of 0.8% per year, rather than the 1.3% per year originally used by Wills. The resultant scale (''TXS,'' for ''Texas Survey'') is about 2% below BW at 365 MHz. For comparison purposes, a reduction was also done using the Cas A spectrum adopted by Baars *et al.* (1977), here denoted ''BA.'' At 365 MHz, the relationship between the three scales is

$$S(\mathrm{TXS})=0.9828S(\mathrm{BW})=0.9607S(\mathrm{BA}).$$

Evaluation of the TXS flux scale at 408 MHz shows it to be identical to the absolute flux scale defined by Wyllie (1969a, 1969b) and used for the Molonglo 408 MHz data.

TABLE 2. Catalog declination strips.

Catalog Strip	Range of declination name	Number of sources	Solid Angle (steradians)	Sources per steradian
−26°	$-357 \le sddd \le -187$	9405	1.634[a]	5731.[a]
−12°	$-186 \le sddd \le -064$	8533	1.314	6494.
−01°	$-063 \le sddd \le +039$	8022	1.139	7043.
+09°	$+040 \le sddd \le +135$	7772	1.039	7480.
+18°	$+136 \le sddd \le +226$	7437	.947	7853.
+27°	$+227 \le sddd \le +316$	6302	.877	7186.
+36°	$+317 \le sddd \le +406$	6367	.796	7999.
+45°	$+407 \le sddd \le +499$	5084	.716	7101.
+55°	$+500 \le sddd \le +598$	4516	.623	7249.
+65°	$+599 \le sddd \le +715$	3403	.523[a]	6488.[a]
TXS	$-357 \le sddd \le +715$	66841	9.607[a]	6952.[a]

[a]Low source density regions below -35°5 (40 sources) and above 71°5 (10 sources) have been excluded from these calculations.

3.3 The Survey

The Texas Survey comprises 66841 sources between declination extrema of −35° 47′ and +71° 35′ (1950 coordinates). Each source is represented by a line in the TXS catalog, and 14964 of the sources have one or more simpler models available, which appear in a separate tabulation of simpler models.

3.3.1 Organization of catalog listings

Each source in the Texas Survey was observed in at least one of the ten observation declination strips, but since observations were naturally made in coordinates of date, the boundaries in 1950.0 coordinates are uneven. Furthermore, in the declination overlap zones the final catalog listing was sometimes chosen from one observation declination strip, and sometimes from the other. The Texas Survey catalog is therefore presented in a series of nonoverlapping *catalog declination strips*, approximately aligned with the observation declination strips, but with fixed boundaries in B1950 declination, as summarized in Table 2.

Each catalog declination strip is predominantly composed of sources from the corresponding observation declination strip, but with sources added from or moved to adjacent strips to fill out to the fixed boundaries. For example, the −12° observation declination strip forms the bulk of the −12° catalog strip listing, but some sources from the −26° and −01° observation strips are included as well, while a few sources from the edge of the −12° observation strip are found in the −26° or the −01° catalog strip listings. The boundaries are established by the declination portion of the source name, which is given in the form HHMM*sddd*, where HHMM are the hours and minutes of B1950 right ascension, and *sddd* refers to the sign and truncated tenths of degrees of declination.

The Texas Survey catalog is presented in Tables 3a–3j, and the corresponding listings of simpler models are in Tables 4a–4j. The first page of Table 3a and the first page of Table 4a, the −26° catalog strip and its associated simpler models, are shown here to give an impression of the entire set of tables, which can be found in the AAS CD-ROM Series.

Each TXS source is represented by one line in one of the ten catalog tables Table 3a–Table 3j. The catalog line is

TABLE 3a. Texas survey, −26° strip.

Source	Code	Right Ascension		Declination		S_{365}		Spec	Var		Structure		(LS)	Obs
0000−322	2+WW	0 0 8.455 ±	.880	−32 15 35.14 ±	19.66	.465 ±	.049	−1.4	.9	116(13)	AD54(34)	-10(7)		A 265
*0000−201	++W	0 0 11.337	.180	−20 11 2.97	2.86	.432	.071 Z	−.3	.4	33(4)	D	-24(12)		A 261
0000−307	C++	0 0 12.473	.065	−30 45 8.77	.83	1.462	.055	−1.6 ± .6	.0X		P		*	A 261
0000−316	CWW	0 0 24.016	.183	−31 36 39.15	3.14	.563	.116 Y	−6.4	4.7X	39(10)	D	100(14)		A 261
0000−334	++W	0 0 31.114	.155	−33 28 37.86	2.44	.518	.084 Z	−.9	1.2	40(5)	D	-7(9)		A 265
0000−277	1++W	0 0 52.238	.204	−27 43 14.43	4.84	.478	.072 Z	.7	4.7X	52(4)	AD26(8)	173(6)		A 265
0000−232	2+CC	0 0 53.184	.531	−23 13 48.73	11.60	.635	.095 Z	−.6	1.3	73(8)	AD43(26)	-29(5)	*	A 261
0000−224	1+WW	0 0 54.663	.201	−22 24 51.89	2.46	.669	.097 Z	1.0	2.1X	55(2)	D	180(4)		A 265
0001−197	2++W1	0 1 2.647	.268	−19 42 18.22	2.04	.549	.092 Z	3.5	.0X	59(4)	D	169(5)	*	A 265
0001−298	CWW	0 1 11.326	.256	−29 50 55.08	2.61	.223	.032 Z	−1.8	1.0X		P			A 261
0001−256	+C+	0 1 13.823	.119	−25 37 5.71	1.00	.562	.060	.6	.7X	30(5)	D	138(8)	*	A 261
*0001−276	1+WW	0 1 14.007	.220	−27 41 4.82	3.87	.464	.065	−2.0	.5	56(4)	AD22(8)	138(4)		A 261
0001−237	+++	0 1 14.441	.037	−23 46 22.80	.49	2.021	.081	−.6 ± .4	1.7	26(1)	D	-6(5)	*	A 261
0001−312	C++	0 1 21.851	.055	−31 16 34.76	.77	2.566	.087	−1.3 ± .5	2.2X		P		*	A 261
0001−273	WWW	0 1 26.369	.181	−27 22 52.85	1.69	.339	.031	−.5	1.9X		P		*	A 261
0001−234A	2NXW	0 1 26.715	.789	−23 24 7.98	13.54	.961	.158 Z	−3.9	5.1X	79(10)	AD48(29)	168(9)		A 265
0001−268	+CC	0 1 27.262	.103	−26 54 1.16	.94	.508	.028	−1.9 ± .8	3.0		P		* (−1,−1)	A 261
0001−333	+WC	0 1 33.608	.160	−33 18 15.95	1.72	.338	.028	−1.1	.3		P		* (+1,−1)	A 265
0001−253	+WW	0 1 34.391	.343	−25 20 28.52	2.10	.285	.047 Z	3.4	1.1	33(6)	D	-101(17)		A 265
0001−347	+++	0 1 38.925	.116	−34 47 49.13	1.10	.767	.042	−.0 ± .8	2.8X		P		*	AA261
0001−224	+++	0 1 43.530	.064	−22 29 34.15	.59	.785	.029	−1.1 ± .6	1.7		P		*	A 261
*0001−289	+++	0 1 47.774	.100	−28 57 4.10	.97	.556	.050	−1.4 ± .8	.7	26(5)	D	-52(10)	*	A 265
0001−234B	1WWW	0 1 48.822	.155	−23 24 15.05	3.09	.917	.096	.8	.8X	57(3)	AD43(7)	179(4)	*	A 265
0002−244	++W	0 2 29.563	.165	−24 28 22.38	1.48	.285	.027	−1.3	1.5		P		* (+1,−1)	A 265
0002−201	++C	0 2 30.438	.104	−20 6 37.52	.80	.584	.034	−2.4 ± .8	.5		P		* (−1,+1)	A 261
0002−189	+CW	0 2 44.107	.271	−18 55 29.72	2.13	.251	.035	.4	2.8X		P		*	AB121
0002−233	+++	0 2 50.851	.071	−23 18 19.71	.74	.702	.030	.3 ± .7	.7		P		*	A 261
0003−257	++W	0 3 .415	.219	−25 45 11.03	2.10	.232	.031	−2.5	4.0		P		*	A 261
0003−199	+++	0 3 14.407	.114	−19 55 52.49	1.32	.585	.077	−2.3	2.4	25(4)	D	11(14)	*	A 261
0003−356	+++	0 3 19.976	.127	−35 38 39.63	1.38	.851	.061	−1.9 ± .8	.9X		P		*	AA261
0003−187	++W	0 3 24.241	.241	−18 42 25.64	1.74	.235	.034 Z	−3.2	1.5		P		*	AB125
0003−282	+++	0 3 25.780	.086	−28 15 44.22	.85	.805	.055	−1.2 ± .7	.7	20(4)	D	-100(19)	*	A 261
*0003−213	++W	0 3 37.984	.290	−21 23 40.71	3.66	.336	.081 Y	.9	4.0	37(6)	D	39(12)		A 261
0004−233	2+++1	0 4 .652	.175	−23 23 56.06	1.68	.416	.063 Z	−7.0	2.2	65(3)	D	161(3)		A 265
*0004−351	++W	0 4 12.109	.198	−35 9 17.43	3.64	.616	.116 Z	6.0	9.3X*	47(5)	D	-15(7)		AA261
0004−244	+++	0 4 16.676	.133	−24 29 44.96	1.21	.312	.026	−3.0	.1		P		*	A 261
0004−258	+++	0 4 36.281	.087	−25 49 38.78	1.02	.550	.030	−.3 ± .8	2.8		P		*	A 261
0004−284	+++	0 4 56.748	.130	−28 25 22.79	1.29	.340	.024	−.9	4.4		P		*	A 261
0005−251	++W	0 5 7.653	.226	−25 9 43.65	2.14	.216	.026	1.8	1.3		P		* (−1,+1)	A 261
0005−309	1++W1	0 5 10.116	.167	−30 59 59.96	3.59	.637	.055	−.1	1.9	50(3)	D	-31(4)	*	A 261
0005−210	+++	0 5 24.167	.126	−21 3 32.71	1.07	.451	.032	−.4	2.7		P		*	A 261
*0005−246	+++	0 5 34.632	.153	−24 36 26.26	2.26	.354	.055 Z	2.4	.7	32(4)	D	-3(12)		A 261
0005−199	++C	0 5 45.830	.079	−19 56 31.41	.72	.721	.037	−2.5 ± .7	.2		P		* (−1,+1)	A 265
0005−262	+++	0 5 53.458	.090	−26 15 53.75	.88	.486	.024	−1.1 ± .8	.6		P		*	A 261
*0006−194	+W+	0 6 23.629	.161	−19 29 14.42	1.61	.498	.076 Z	−.8	.4	31(5)	D	-40(10)		A 261
0006−212	+++	0 6 33.158	.049	−21 13 14.19	.48	1.261	.039	−.4 ± .5	3.5		P		*	A 265
0006−286	+WW	0 6 50.808	.091	−28 38 35.15	.96	.983	.070	−.8 ± .8	2.3X	30(3)	D	-114(7)	* (+2,+0)	A 261
0006−320	WW+	0 6 52.109	.088	−32 2 57.57	.97	1.220	.057	−2.0 ± .7	1.0X		P		*	A 265
*0006−355	1++W	0 6 52.560	.306	−35 32 51.99	4.61	.841	.149 Z	−1.5	4.0X	66(7)	AD36(11)	-140(5)	*	AA261
*0006−249	++C	0 6 53.163	.106	−24 56 54.31	1.68	.541	.059	−.5	1.7	35(3)	D	10(7)	* (−1,−1)	A 265
0007−325	NWC	0 7 3.391	.167	−32 33 19.46	2.01	.855	.130 Z	.5	3.9X	31(8)	D	146(14)	*	A 265
0007−264	+++	0 7 10.870	.171	−26 26 26.69	1.64	.252	.023	−1.1	1.1		P		*	A 261
0007−317	WWW	0 7 12.778	.252	−31 43 50.32	2.84	.666	.123 Z	−.9	.4X	38(5)	D	-112(11)	(−1,−1)	A 265
0007−287	+WC	0 7 23.706	.122	−28 46 8.52	.75	1.289	.068	−.7 ± .7	.8	38(2)	D	-101(5)	* (−1,−1)	A 261
*0007−235	+++	0 7 32.364	.085	−23 33 28.94	.74	.725	.058	−2.3 ± .7	.0	26(4)	D	53(7)	*	A 261
0007−296	1+WW1	0 7 40.147	.162	−29 36 9.90	1.79	.600	.073	−5.0	.1X	47(3)	D	-46(4)	*	A 265
*0007−282	++W	0 7 53.929	.367	−28 12 25.38	1.69	.284	.032	.8	.5	37(5)	D	93(13)	* (+2,+0)	A 261
0008−311	+WW	0 8 2.944	.134	−31 10 55.60	1.98	.523	.070	−.8	3.2X	33(5)	D	-168(11)	* (+1,+1)	A 265
0008−307	NWW	0 8 3.578	.168	−30 44 27.70	1.97	.467	.044	.6	.0X		P		*	A 261
*0008−192	+++	0 8 5.662	.059	−19 16 17.86	.72	1.312	.087	−.7 ± .6	.5	23(2)	D	19(8)	*	A 265
0008−326	WCW	0 8 6.435	.106	−32 41 49.86	1.30	.849	.062	−4.7	.6X		P		* (−1,−1)	A 261
*0008−257	+++	0 8 8.247	.135	−25 44 20.52	1.16	.421	.046	−1.2	.6	26(6)	D	-62(12)	*	A 261
0008−343	1+WW	0 8 19.780	.257	−34 22 41.92	5.24	.640	.079	−.1	.8X	80(4)	AD34(9)	-178(3)		AA261
0008−222	+++	0 8 21.062	.097	−22 13 44.19	.85	.508	.027	−.1 ± .9	.2		P		*	A 261
*0008−264	+++	0 8 28.906	.147	−26 29 12.20	1.16	.414	.035	.8	12.9 *	26(5)	D	83(16)	*	A 261
0008−299	+WW	0 8 30.287	.181	−29 54 12.53	1.96	.244	.025	−1.5	.2		P			A 265
0008−321	+++	0 8 41.505	.062	−32 7 10.94	.80	1.527	.096	−1.3 ± .6	.8	17(6)	D	-133(19)	*	A 265
0008−215	+++	0 8 45.060	.142	−21 32 53.86	1.26	.334	.027	−1.4	.1		P		*	A 261
0009−242	+++	0 9 5.153	.070	−24 15 59.76	.75	.738	.032	−.7 ± .6	.8		P		*	A 261
0009−219	+++	0 9 5.749	.269	−21 54 15.16	2.26	.176	.027 Z	−2.2	.1		P			A 261

Table 3 is presented in its complete form in the AAS CD-ROM Series, Vol. 6, 1996.

explained in full detail in the Appendix, but is briefly summarized here. The source name, which in external references should be preceded by the letters TXS, is followed by a column of quality flags, and then by the B1950 right ascension and declination of the *centroid* of the source with associated internal error. The 365 MHz flux density in Jy and its internal error is followed by the internally estimated spectral index (and its error, if the estimate is accurate enough to be worthy of attention). The variability parameter which is in the next column is the standardized squared residual of the flux density of the source at the four observing epochs; values larger than about 13 suggest source flux variability. The next field contains the source structure model which best fits the data. The validity of the parameters and errors in all

TABLE 4a. Simpler models, −26° strip.

Source	Code	Right Ascension		Declination		S_{365}		Spec	Var	Structure			(LS)	Obs
0000−201	++W	0 0 11.351 ±	.216	−20 11 3.69 ±	2.34	.272 ±	.038	−.3			P			A 261
0001−276	1+WW1	0 1 13.643	.232	−27 40 57.63	3.33	.417	.071 Z	−2.0		48	D	141		A 261
0001−289	+++	0 1 47.771	.098	−28 57 4.02	1.02	.466	.026	−1.4 ± .8			P			A 265
0003−213	++W	0 3 37.939	.353	−21 23 40.18	3.23	.160	.036 Y	.9			P			A 261
0004−351	++W	0 4 12.094	.316	−35 9 18.29	3.37	.273	.043 Z	6.0			P			AA261
0005−246	+++	0 5 34.622	.215	−24 36 26.03	1.91	.206	.024	2.4			P			A 261
0006−194	+W+	0 6 23.594	.196	−19 29 14.59	1.53	.322	.035	−.8			P			A 261
0006−355	++W	0 6 53.107	.302	−35 32 43.37	2.90	.601	.151 X	−1.5		41	D	-155		AA261
0006−355	++W	0 6 53.230	.399	−35 32 43.49	2.76	.377	.055 Z	−1.5			P			AA261
0006−249	++C	0 6 53.126	.165	−24 56 53.59	1.60	.306	.031	−.5			P			A 265
0007−235	+++	0 7 32.354	.084	−23 33 28.96	.77	.592	.029	−2.3 ± .7			P			A 261
0007−282	++W	0 7 53.815	.209	−28 12 24.75	2.09	.210	.023	.8			P			A 261
0008−192	+++	0 8 5.663	.067	−19 16 17.96	.81	1.082	.058	−.7 ± .6			P			A 265
0008−257	+++	0 8 8.241	.122	−25 44 20.46	1.21	.350	.024	−1.2			P			A 261
0008−264	+++	0 8 28.908	.125	−26 29 12.46	1.32	.354	.025	.8			P			A 261
0009−325	+W+	0 9 21.431	.063	−32 31 39.46	.85	1.005	.037	.5 ± .6			P			A 265
0009−231	+++	0 9 47.207	.140	−23 10 58.78	1.23	.344	.030	−3.1			P			A 261
0009−218	+++	0 9 57.289	.171	−21 49 23.93	1.44	.283	.028	−1.6			P			A 265
0010−237	++C	0 10 20.255	.070	−23 44 .66	.68	.751	.033	−1.0 ± .6			P			A 261
0010−283	+CW	0 10 49.977	.208	−28 18 27.39	2.01	.223	.026	−.8			P			A 265
0011−352	+++	0 11 6.216	.165	−35 12 53.98	1.53	.571	.038	1.1			P			AA261
0011−326	++C	0 11 8.339	.114	−32 41 26.33	1.15	.826	.062	−.7 ± .8		34	D	118		A 261
0012−247	2++C1	0 12 3.442	.222	−24 45 2.47	1.30	.717	.068	−1.7 ± .8		76	D	175		261
0013−197	+++	0 13 27.778	.034	−19 46 1.97	.40	2.253	.053	−1.4 ± .4			P			261
0013−240	+++	0 13 33.707	.132	−24 0 29.96	1.17	.363	.026	−.3			P			261
0014−234	+++	0 14 8.780	.138	−23 28 17.18	1.21	.329	.025	−.5			P			261
0014−228	+WW	0 14 33.428	.144	−22 51 49.21	1.29	.326	.029	−2.8			P			261
0015−229	+++	0 15 26.473	.048	−22 54 44.34	.45	1.166	.032	−.8 ± .4			P			261
0016−223	+++	0 16 51.266	.129	−22 22 5.35	1.17	.430	.032	−.9			P			261
0017−342	++W	0 17 58.171	.262	−34 13 9.01	2.38	.277	.031	1.8			P			A261
0018−251	+++	0 18 29.144	.068	−25 7 35.89	.61	.723	.025	.1 ± .6			P			261
0018−194	+++	0 18 41.540	.038	−19 27 22.49	.38	2.458	.113	−.1 ± .3		8	D	52		261
0018−194	+++	0 18 41.541	.037	−19 27 22.48	.37	2.421	.057	−.1 ± .3			P			261
0019−339	+WC	0 19 51.310	.167	−33 56 49.14	1.64	.433	.034	.3			P			261
0021−213	+++	0 21 10.858	.119	−21 21 25.28	1.01	.466	.032	−1.9 ± .9			P			261
0022−189	++W	0 22 21.329	.228	−18 56 21.40	1.42	.259	.039 Z	−4.6			P			B121
0022−279	+WC	0 22 28.331	.155	−27 54 57.86	1.28	.367	.027	−.8			P			261
0023−223	+CC	0 23 52.710	.128	−22 19 28.59	1.08	.535	.036	2.3			P			261
0024−340	+++	0 24 50.236	.070	−34 3 23.78	.78	1.250	.043	.4 ± .5			P			A261
0024−212	+CW	0 24 57.085	.166	−21 12 2.40	1.42	.308	.028	−.5			P			261
0024−277	+++	0 24 59.549	.042	−27 47 46.15	.60	1.501	.045	−1.5 ± .4			P			261
0025−286	+W+	0 25 40.865	.143	−28 40 55.57	1.29	.474	.053	−1.0		27	D	-57		261
0025−215	++C	0 25 54.511	.195	−21 30 26.48	1.60	.253	.025	1.4			P			261
0028−223	+++	0 28 32.322	.050	−22 23 40.87	.50	1.011	.030	−1.0 ± .5			P			261
0029−214	+++	0 29 29.089	.101	−21 26 12.34	.81	.605	.032	−.1 ± .7			P			261
0030−280	+C+	0 30 9.902	.139	−28 5 43.63	1.38	.327	.023	−.9			P			261
0030−331B	+WW	0 30 50.290	.137	−33 11 3.25	1.99	.559	.070	1.7		38	D	-157		261
0031−257	+WC	0 31 7.604	.111	−25 44 5.80	1.04	.447	.028	−2.3 ± .9			P			261
0032−218	+W+	0 32 .840	.101	−21 50 22.17	.96	.475	.029	−2.6 ± .9			P			261
0033−279	+++	0 33 15.220	.109	−27 54 36.62	1.14	.443	.027	−.3 ± .9			P			261
0033−255	+++	0 33 24.864	.146	−25 31 18.07	1.42	.287	.023	−2.3			P			261
0033−267	++W	0 33 31.247	.087	−26 42 24.06	.93	.548	.028	−.8 ± .8			P			261
0034−320	++W	0 34 26.728	.164	−32 1 3.17	1.77	.307	.026	.9			P			261
0034−304	+++	0 34 59.665	.128	−30 29 8.48	1.40	.331	.023	.0			P			261
0036−216	+C+	0 36 .337	.049	−21 36 34.36	.48	1.198	.034	.3 ± .5			P			261
0036−308	+++	0 36 20.496	.101	−30 51 14.00	1.21	.537	.030	.9 ± .8			P			261
0037−336	+++	0 37 2.022	.080	−33 39 5.70	.97	.774	.032	−1.5 ± .7			P			261
0039−280	+++	0 39 26.595	.067	−28 5 25.65	.75	.841	.032	.1 ± .6			P			261
0040−349	++W	0 40 9.325	.139	−34 55 57.41	1.37	.682	.102 Z	−1.9 ± .9		16	D	175		A261
0040−349	++W	0 40 9.334	.141	−34 55 57.60	1.33	.624	.038	−1.9 ± .9			P			A261
0040−194	+++	0 40 34.935	.085	−19 24 41.58	.71	.752	.037	−1.5 ± .7			P			261
0041−302	++W	0 41 6.345	.220	−30 17 2.84	2.15	.209	.030 Z	−5.1			P			261
0042−253	++W	0 42 18.813	.167	−25 20 58.55	1.50	.312	.027	−.8			P			261
0042−218	++C	0 42 27.103	.196	−21 50 4.52	1.84	.254	.039 Z	−3.8			P			261
0043−198	+++	0 43 49.790	.201	−19 50 35.24	1.89	.264	.033	−1.5			P			261
0044−229	+++	0 44 19.176	.118	−22 59 20.54	.95	.768	.071	−.6 ± .8		32	D	-119		261
0044−312	++C	0 44 29.854	.107	−31 13 33.04	1.11	.450	.025	−1.3 ± .8			P			261
0044−329	+CW	0 44 49.203	.189	−32 56 23.73	3.88	.601	.078	2.7		47	D	154		261
0046−221	++W	0 46 .303	.142	−22 9 13.46	1.30	.364	.029	−1.9			P			261
0046−227	++C	0 46 28.029	.158	−22 46 56.04	1.49	.291	.026	.5			P			261

Table 4 is presented in its complete form in the AAS CD-ROM Series, Volume 6, 1996.

previous columns is subject to the correctness of this model. Finally, a field of comments follows, including possible lobeshift positions and reference to the observation strip from which this catalog line was taken.

4. PROPERTIES OF THE SURVEY

4.1 Completeness

We define completeness above flux density S as that fraction of sources with true flux density greater than S which appear in the catalog; the corresponding differential completeness is the fraction of sources with true flux density S which appear in the catalog.

Three general factors contribute to incompleteness in the Texas Survey: First, there is a noise limitation (the Survey is noise rather than confusion limited). Sources with flux densities below a few hundred mJy will definitely be missed, since to be included a source must have appeared in a number of FINDER catalogs, which themselves are noise limited.

TABLE 5. Survey completeness comparison.

	Limiting flux(Jy at 408 MHz)				
Declination Strip	0.25	0.35	0.50	0.75	1.00
Central Zone[a]	0.82 (0.50)[b]	0.89 (0.75)	0.93 (0.88)	0.96 (0.94)	0.96 (0.95)
−12°, +65°	0.79 (0.37)[c]	0.89 (0.64)[c]	0.93 (0.88)[c]	0.96 (0.94)	0.96 (0.95)
−26°	0.69 (0.23)	0.83 (0.55)	0.88 (0.78)	0.94 (0.87)	0.93 (0.93)

[a]This includes the 7 declination strips from −01° through +55°
[b]integral(differential)
[c]estimate based on interpolation using Survey n(S)

Second, *obscuration* produces incompleteness, since close (<10′) pairs are generally counted as one (poorly modeled) source. Sources at even wider spacings can be affected if one is significantly stronger than the other. Finally, *resolution* will play a role: sources with component sizes on the order of 30″ have a fringe visibility of 0.5 on even the shortest baselines, and thus appear with half their true flux density, while those with component sizes greater than about 1′ are strongly resolved and seen at greatly reduced amplitude, if at all.

All three factors may vary with the declination strip: the sensitivity of different strips varies slightly, but more importantly, with foreshortening at large zenith angles increasing the primary beam size and decreasing the fringe spacing, the effects of obscuration and resolution will differ. Inspection of the differential source surface density for the different strips shows that the central zone of the survey (the seven declination strips from −01° through +55°) is remarkably homogeneous, while the outer strips have significantly fewer sources at low flux density than the central region.

The completeness of the Survey can be assessed directly when a comparison catalog of known reliability is available at or near the Survey frequency. The fraction of comparison catalog sources with flux density S which appear in the Survey is the product of the comparison catalog reliability at S and the completeness of the Survey at flux density S. Such a comparison was made with the *Molonglo Reference Catalog* (MRC: Large *et al.* 1981) down to a 408 MHz flux density of 0.75 Jy, with MC2, MC3 (Sutton *et al.* 1974) and B2.4 (Fanti *et al.* 1974) down to 0.5 Jy, and with MC1 (Davies *et al.* 1973) and the first three sections of the B2 Survey (Colla *et al.* 1970, 1972, 1973) down to 0.25 Jy. The flux densities in these catalogs were placed on the scale of the *Molonglo Reference Catalog* (using correction factors given by White 1983), and integral and differential completeness values were obtained at a series of 408 MHz flux densities with results shown in Table 5.

Table 5 lists the integral completeness, followed in parentheses by the differential completeness; where direct comparison data were unavailable (three cases) the entries are based on an interpolation using the Survey source density. The central zone of the Survey is about 0.82 complete above 0.25 Jy; completeness and homogeneity among the strips rises with flux density, as expected, and above 0.75 Jy all declination strips have integral completeness of 0.95. These flux densities refer to 408 MHz; if one presumes that the majority of sources have the usual steep spectral index, integral completeness would be 0.82 at 0.28 Jy at 365 MHz, 0.89 at 0.39 Jy—in round numbers, about 0.8 at 0.25 Jy and 0.9 at 0.40 Jy.

A number of the strongest sources in the sky do not appear in the Texas Survey. The dynamic range of the telescope is limited—sources with fringe amplitude greater than about 100 cos δ Jy are off-scale—and those strong sources whose fringe amplitude does remain on-scale does so because of great angular size and reduced fringe visibility. Fourteen of the 18 brightest 3CR sources are not in the Survey, and the other 4 are so heavily resolved as to be useless; among the 44 next-brightest 3CR sources seven are missing. Most of the missing sources are galactic objects of large angular size. Robertson (1973) prepared an all-sky catalog of extragalactic ($|b|>10°$) sources brighter than 10 Jy at 408 Mhz; 34 of these are brighter than 20 Jy at 408 MHz, and 7 of these 34 brightest are missing from the Survey, and two further are so heavily resolved as to be useless. Thus, for example, Cas A, Cygnus A, Virgo A, 3C 123, 3C 147, 3C 295, 3C 348 are not in the Survey. Other well-known strong sources may be present but at greatly reduced amplitude due to resolution—such as the 150 Jy source 3C 353, which appears in the Survey as an 18 Jy heavily resolved source. A rerun with attenuators was deemed to be inadvisable since many are known to be so large as to be poorly modeled by the system.

4.2 Reliability

Reliability is the probability that a catalog source corresponds to a true source in the sky, having the parameters given within the listed errors. This may be further represented as the product of *enumeration reliability* (the probability that a source of approximately this flux density is approximately in this direction) and *characterization reliability* (the probability that a correctly enumerated source is correctly described, e.g., is at the right position and structure lobe).

4.2.1 Enumeration reliability

One straightforward way to assess the enumeration reliability of the Texas Survey is to compare it, or portions of it, with other surveys at comparable frequencies and epochs which go as deep or deeper than the flux level at which the assessment is made. The fraction of TXS sources which also appear in the comparison catalog is the product of the reliability of the TXS catalog and the completeness of the comparison catalog (with of course the small adjustments required for random coincidences).

This can be done for strong sources using many published catalogs. There are 834 sources in the Texas Survey with 365 MHz flux density greater than 4.0 Jy. The MRC catalog is complete (outside the galactic plane) to about 1 Jy, and can be used below +18°; many northern hemisphere catalogs are available going that faint or fainter. This strong source sample is confirmed in 830 cases, and in 4 cases no confirmation has been found. One source (TXS 2310+593) is near Cas A but is otherwise normal in appearance; perhaps it has been lost in Cas A sidelobes until now. A second source (TXS 0848−346) is in the southern hemisphere galactic plane, where the MRC catalog does not venture, and is probably real. A third source (TXS 0427−345) is at the same

TABLE 6. Enumeration reliability.

S_{lim}	N_{TXS}	N_{conf}	$N_?$	N_X	$R\times C$	R_{max}	Comparison
4.0	834	830	3	1	0.995	0.999	All-sky, strong source
2.0	1738	1717	19	2	0.988	0.999	MRC overlap region
1.2	4288	4154	128	6	0.969	0.999	MRC overlap region
0.1	2271	2249	7	15	0.990	0.993	Arecibo +18° sub-region

right ascension as a much stronger MRC source, and may have been missed by MRC. The fourth source, TXS 1828 +474, is probably spurious. Thus, one of the brightest 834 sources in the Survey is probably spurious.

A second comparison for sources brighter than 2 Jy at 365 MHz was made, using the area of the sky which overlapped the MRC, omitting low galactic latitudes, and a third was made using the same overlap region, but including Texas sources down to 1.2 Jy, which corresponds to the 1 Jy lower bound of ''completeness'' of the MRC.

Enumeration reliability assessment for the weakest sources requires another procedure: a special observing program in which a series of sources are examined in turn with an instrument capable of going deeper than the survey. Such an observing program was carried out by Douglas & Davis (1981) at Arecibo (at 1400 MHz), in which the field of each of a complete sample of 2271+18° strip sources was examined; no source was found in 15 cases, and the results were inconclusive in 7 cases.

The results of these four comparisons are shown in Table 6. The $R\times C$ column assumes both the questionable ($N_?$) and the definitely spurious (N_X) sources are bad; the $R_{\rm max}$ column takes the number of bad sources as being N_X. We can conclude that the reliability of the Texas Survey in both flux-limited samples and in the Survey as a whole is better than 0.99, and incidentally that the completeness of the MRC must be about 0.98 at 1 Jy at 408 MHz.

4.2.2 Characterization reliability

Position or structure lobeshifts can cause the listed position and flux density of sources to to deviate by amounts grossly exceeding the quoted error. Such errors are bound to be more common for weak sources than for strong ones, and more common for sources whose baseline fringe amplitude is affected by nearby sources or by the failure of the source to approximate the only type of model that we fit: the asymmetric double source.

Assessment of lobeshift errors requires a comparison observation whose position error is small compared to the lobe spacing, i.e., small compared to 50 arcsec when position lobeshifts are considered, and small compared to 25 arcsec when the possibility of structure lobeshifts is under consideration. Thus, we can confirm lobe choice when, e.g., VLA maps are available, but systematic catalogs with the necessary accuracy to investigate structure lobe shifts are limited to the stronger sources.

Table 7 presents the results of a number of comparisons at different flux levels for the subgroups expected to exhibit the best (model, environment and lobeshift flags all ''+'') and the worst (lobeshift flag set to Warning ''W'') behavior, and for the sources which fall in between. The comparison sources have been taken from the Molonglo catalogs, and for the subset of the 87GB catalog sources (Gregory & Condon 1991) which have position accuracy better than 15 arcsec. The numbers in Table 7 are the probability that the listed model is centered, requiring neither a position nor a structure lobeshift; the numbers following in parentheses are the fraction of sources in the entire TXS which fall into this class. Based on Table 7, one can say roughly 1/4 of sources have a lobeshift risk of 1%–2%; roughly 1/4 have a lobeshift risk of 40%, and half the sources have a lobeshift risk of about 10%. A source may be assigned to these groups based on the Code Field flags.

TABLE 7. Characterization reliability.

Code Field	Model	$S_{365}<0.5$ Jy	$0.5<S<1.0$ Jy	$S>1.0$ Jy
No Adverse Flags	Point	0.942 (0.1221)	0.976 (0.0677)	0.987 (0.0330)
	Double	0.884 (0.0433)	0.938 (0.0774)	0.970 (0.0495)
	ADouble	0.611 (0.0019)	0.794 (0.0075)	0.845 (0.0139)
Lobeshift Warning	Point	0.678 (0.1494)	0.782 (0.0050)	0.8 (0.0004)
	Double	0.514 (0.1008)	0.528 (0.0036	0.590 (0.0050)
	ADouble	0.3 (0.0172)	0.42 (0.0203)	0.503 (0.0101)
All Others	Point	0.912 (0.0887)	0.937 (0.0207)	0.973 (0.0083)
	Double	0.783 (0.0430)	0.863 (0.0388)	0.934 (0.0207)
	ADouble	0.6 (0.0033)	0.657 (0.0081)	0.658 (0.0103)

4.3 Accuracy

All errors quoted on the catalog lines are internal (discussed in Sec. *4.3.1*) and do not include the uncertainty of relating the survey position system to the position or flux system defined by the calibrators (calibration error), nor do they include any estimates of other sources of error, such as position centroid variance when the source is observed at different frequencies, or uncompensated systematic errors in the position or flux system.

To obtain the best estimate of the error of a source position or flux density relative to the adopted position and flux system, the internal errors on the catalog line should be added in quadrature with the calibration error (Sec. *4.3.2*); the change is negligible except for the stronger sources.

External comparisons (Sec. *4.3.3*) however show that there is more scatter in the position and flux residuals than expected from the quadratic sum of Survey and external catalog errors; this excess error should also be added in quadrature if one takes the point of view that the error is in the Texas Survey rather than in the comparison catalog.

4.3.1 Internal errors

The internal errors are calculated from the the covariance matrix of the least-squares adjustment which produced the model listed, using the appropriately propagated baseline noise or the observed standard deviation of unit weight obtained from the residuals to the overdetermined solution, whichever is larger. The correctness of the internal error calculation procedures for all parameters (position, flux, spectrum, double separation, position angle, and source flux ratio) has been verified by extensive Monte Carlo testing,

TABLE 8. Survey average internal errors.

Model	σ_S (Jy) .25 Jy	.5 Jy	1.0 Jy	$\sigma_{\alpha \cos \delta}$ ($''$) .25 Jy	.5 Jy	1.0 Jy	$\sigma_{\delta \cos z}$ ($''$) .25 Jy	.5 Jy	1.0 Jy
Point	.0246	.0252	.0273	2.085	1.069	0.585	0.860	.450	.262
Double	.0495	.0503	.0535	2.833	1.430	0.742	1.390	.703	.366
Adouble	.0520	.0528	.0556	4.771	2.452	1.352	3.782	1.932	1.043

which also confirmed that the variability parameter has the expected χ-squared distribution with two degrees of freedom.

Internal errors for individual sources should of course be taken from the catalog listing; however, one can characterize the average behavior to give a feeling for the internal accuracy attained by the Survey. The average errors expected should of course depend on flux density, declination of the source (we should expect the error in $\alpha \cos \delta$ and $\delta \cos z$ to be approximately comparable over the sky), and on the model chosen, being substantially worse when D or AD models are listed.

The actual average internal position and flux errors for the three structure types for the Survey as a whole, calculated for flux densities of 0.25, 0.5, and 1 Jy, are given in Table 8. Note that the right ascension error is systematically about twice as great as the declination error. This is an expected result of the Texas Interferometer baseline arrangements: the largest E-W component used is 2000 wavelengths, while the largest N-S baselines have 4000 wavelength spacing. The larger errors in the D and AD models are of course in part due to the larger number of parameters in these cases, but principally arise from the covariance of position and flux estimates with the structure models themselves and the fact that the total flux density at which the error is evaluated corresponds to a lower fringe amplitude and thus lower signal to noise ratio.

Internal errors for the separation and position angle of double sources are listed on each catalog line, together with errors in the flux ratio parameter for asymmetric doubles. These errors covary with the flux density and position errors and with each other, and depend on the orientation and separation of the double. And while flux and position values are relatively insensitive to small deviations in the actual brightness distribution of the source from the model adopted, the model parameters themselves of course can be significantly affected. Examination of the quoted errors for separation and position angle for those double sources which are above median signal-to-noise ratio and which have no adverse flags (i.e., are +++ sources) shows that half have internal errors in the quoted separation of less than 2 arcsec, and 84% less than 3 arcsec, and that in half the cases, internal error in the quoted position angles are between 5° and 14°.

4.3.2 *Calibration error*

Calibration error was not included in the catalog listing for each source. This error is calculable from the covariance matrix and the standard deviation of unit weight of the reduction to sky process, and represents the accuracy with which the position or flux system of an observed declination strip has been reduced to the position and flux systems defined by the position and flux calibrator adopted values. For each declination strip the set of residuals $\Delta\alpha \cos \delta$, $\Delta\delta$, $\Delta \log S$ to flux or position calibrators is fit to a series of systematic error models having parameters C_i, $i=1$, m, where the number of parameters m is successively 1,2,4,6,8,10. For $m=1$, only a position offset or additive factor in $\log S$ is considered; $m=2$ includes a systematic slope in declination; and higher values of m include cosine and sine terms of up to four periods (24, 12, 8, and 6 h) of right ascension variation. The full systematic error equation for right ascension, for example, is

$$\Delta \alpha \cos \delta = C_1 + C_2 \delta + \sum_{k=1}^{4} (C_{1+2k} \cos k\alpha + C_{2+2k} \sin k\alpha).$$

TABLE 9. Calibration error.

Observation Strip	Right Ascension ($\alpha \cos \delta$; $''$) n	m	σ_c	Declination (δ; $''$) n	m	σ_c	Flux ($\ln S$) n	m	σ_c
−26°	79	4	0.261	77	10	0.505	80	1	0.006
−12°	73	1	0.107	73	8	0.316	62	1	0.006
−01°	66	8	0.236	66	6	0.216	80	1	0.007
+09°	71	8	0.205	71	8	0.155	71	10	0.025
+18°	101	8	0.189	101	6	0.157	87	1	0.007
+27°	109	8	0.216	105	10	0.243	64	1	0.007
+36°	172	10	0.170	166	8	0.132	82	4	0.015
+45°	144	8	0.180	142	4	0.104	39	2	0.017
+55°	123	1	0.065	125	6	0.169	22	1	0.013
+65°	106	1	0.125	111	6	0.169	23	1	0.019

The least complicated such model showing significant improvement as judged by an F test was adopted for right ascension correction for that declination strip.

Similar fits were carried out for declination and $\log S$. There are thus three fits for each declination strip, or 30 in all. In 10 cases it was not deemed worthwhile to go beyond the simplest model in which only the C_1 term was used, while in other cases m for the solution chosen ranged from 2 to 10. There are instrumental reasons to expect small systematic terms in the form proposed for position and flux in all strips. It should be noted that adopting a fit with $m=1$ does not mean that the quantity involved has no systematic error in declination or right ascension in the declination strip in question, but rather that any such variation cannot established with the available calibrator set, either because of a limited number or poor distribution of calibrators, or because the systematic effects themselves are small compared to the errors in the residuals, or both.

Texas Survey catalog lines have been corrected to sky using the results of these 30 fits, and the calibration error (or average calibration error, where $m>1$ and the error varies over the strip) is summarized in Table 9. The number of calibrators actually used in each fit is n, the number of parameters in the fit chosen is m, and the calibration errors are standard deviations that should be added in quadrature to the errors listed in the catalog line to reflect our best estimate of the error of a given source relative to the position and flux systems adopted. This addition will make a negligible change in the errors of all but the stronger Survey sources.

4.3.3 External errors

The most readily accessible large groups of sources for external comparisons are the calibrator sets themselves. The calibration solutions are so heavily overdetermined that the residuals of the calibrated survey to the calibrators are a fair test of the external accuracy of the Survey, although not of course of the accuracy of the position and flux systems which the calibrators themselves define.

We wish to discuss the external accuracy of sources which have been properly characterized in the sense discussed above, i.e., sources which are listed at the correct position and structure lobe. We will concentrate on sources which are free of catalog line warnings which suggest or ensure accuracy worse than quoted, such as sources with C, W, or N model flags, and sources with C, W, or X environment flags. Even with such restrictions, we expect to find that whatever the basic residual distribution, there will be wings of occasional excessive deviation caused by Survey errors, or by comparison source errors, or both.

Position error. The Survey includes catalog lines for 1852 sources which are in the position calibrator list (as described in Sec. *3.2.1* above). Removing those catalog lines whose model and environment flags are not both "+" reduces the sample to 1383 sources, while the subsequent removal of all "AD" model sources results in a sample of 1225 sources whose position accuracy we should expect to be nominal. However, in 27 cases the source model chosen appears to be position or structure lobeshifted; removing these leaves an external comparison sample of 1198 sources from the position calibrator list.

Residuals $\Delta l \equiv (\alpha_{\rm cal} - \alpha_{\rm TXS}) \cos \delta_{\rm TXS}$ and $\Delta m \equiv (\delta_{\rm cal} - \delta_{\rm TXS}) \times \cos(\phi - \delta_{\rm TXS})$ were calculated in arcsec; the cosine of the zenith distance was included in Δm to increase homogeneity across the declination strips, in view of the foreshortening of the N-S baselines. The internal standard deviation of each residual was taken to be the quadratic sum of the internal Survey error listed on the catalog line and the quoted calibrator error. The average of the standard deviations of the residuals in this set of 1198 sources was 1.15 arcsec in Δl, 0.83 arcsec in Δm. Interpreting the range between the first and third quartiles of the sample of 1198 residuals in terms of standard deviation of a underlying Gaussian distribution gives a sample standard deviation of 1.16 arcsec in Δl, 0.88 arcsec in Δm.

This agreement is satisfactory, but can conceal excess errors at the level of several tenths of an arcsecond. Accordingly, a subset containing 196 of the position calibrator sources having an internal standard deviation of the residual Δm of less than 0.3 arcsec was examined. The sample standard deviation of this group by the quartile method was 0.55 arcsec in Δl (compared to an average error of 0.36 arcsec), and 0.42 arcsec in Δm (compared to an average error of 0.20 arcsec). This is consistent with the presence of an underlying excess error of 0.4 arcsec in $\Delta \alpha \cos \delta$ and in $\Delta \delta$, together with calibration error discussed above.

Taking the error of each residual to be the quadratic sum of the catalog line error, the calibrator error, the calibration error, and the 0.4 arcsec excess error, weighted means of Δl and Δm were calculated for each declination strip, together with the standard error of the mean and the standard deviation of unit weight. Outliers with vector deviations greater than 2.83 σ (the 0.1% level) were discarded in the calculation. The results are given in Table 10 (the high-accuracy group of 196 sources) and Table 11 (the entire group of 1198 sources). Note that 20 of the 196 sources in the 0.3 arcsec group were discarded because of excessive deviation, and 89 of the 1198 sources in the position calibrator group were discarded. None of the means in the larger group is significantly different from zero; however, in the 0.3 arcsec group there is a suggestion (contradicted by the larger group) that the survey position system is nearly 0.1 arcsec too high in declination.

The excess variance of 0.4 arcsec is not due to errors in the calibrator source positions; the calibrators involved all have radio astrometric positions of far better accuracy than this. A portion is certainly a result of the difference between the 365 MHz and high-frequency radio centroid of extended sources ("centroid variance"); but a portion may also be due to small remaining periodic errors in the Survey.

Flux density errors. The 582 sources used to calibrate the Survey flux density scale have already been preselected to avoid bad models, nearby interfering sources, or lobeshifts. The residuals Δr were formed as the natural logarithm of the ratio of the calibrator flux density to the Survey flux density; the error of each residual was obtained by the quadratic sum of the fractional errors quoted on the catalog line and of the calibrator source. The average error of the 582 residuals is 0.029, while the standard deviation of the residuals, estimated from the range between first and third quartiles, is 0.064. There is thus an average excess error of just over 5% in this data set. Using an excess error of 0.05, 11

TABLE 10. Weighted mean residuals, 0.3 arcsec group.

Catalog Strip	Right Ascension $\overline{\Delta l}('')$	$\sigma_{\overline{\Delta l}}('')$	σ_{uw}	Declination $\overline{\Delta m}('')$	$\sigma_{\overline{\Delta m}}('')$	σ_{uw}	Number of sources
−26°	0.220	0.144	1.080	−0.004	0.096	0.905	18
−12°	0.294	0.178	0.985	−0.037	0.129	1.035	11
−01°	0.095	0.139	0.642	0.029	0.104	1.063	16
+09°	0.066	0.117	0.704	−0.020	0.091	0.738	24
+18°	−0.125	0.114	0.868	−0.233	0.096	0.829	22
+27°	−0.093	0.159	0.844	−0.223	0.133	1.177	14
+36°	−0.011	0.094	0.811	−0.154	0.083	1.113	29
+45°	0.136	0.142	0.636	−0.143	0.113	1.230	16
+55°	0.264	0.150	1.231	−0.116	0.130	0.722	12
+65°	0.016	0.142	1.331	0.080	0.126	0.735	14
TXS	0.043	0.042	0.940	−0.084	0.033	0.997	176

TABLE 11. Weighted mean residuals, position calibrations.

Catalog Strip	Right Ascension $\overline{\Delta l}('')$	$\sigma_{\overline{\Delta l}}('')$	σ_{uw}	Declination $\overline{\Delta m}('')$	$\sigma_{\overline{\Delta m}}('')$	σ_{uw}	Number of sources
−26°	0.025	0.110	1.160	−0.099	0.070	1.190	73
−12°	0.226	0.120	1.099	0.015	0.087	1.138	66
−01°	0.093	0.094	1.000	−0.027	0.068	1.163	79
+09°	0.065	0.081	1.065	−0.038	0.064	1.074	90
+18°	−0.087	0.075	1.051	0.028	0.063	1.047	103
+27°	−0.105	0.095	1.046	0.009	0.072	1.093	132
+36°	−0.034	0.062	0.942	0.080	0.054	0.938	192
+45°	0.015	0.089	1.037	−0.033	0.072	1.102	146
+55°	0.081	0.092	1.151	−0.036	0.077	1.031	135
+65°	0.114	0.106	1.267	−0.141	0.087	1.088	93
TXS	0.018	0.028	1.075	−0.013	0.022	1.073	1109

TABLE 12. Weighted mean residuals, flux calibrations.

Catalog Strip	Excess error	$\overline{\Delta r}$	$\sigma_{\overline{\Delta r}}$	σ_{uw}	Number of sources
−26°	0.040	0.001	0.006	1.084	80
−12°	0.030	0.000	0.006	1.001	61
−01°	0.050	0.000	0.006	1.061	80
+09°	0.030	0.004	0.006	1.040	67
+18°	0.050	0.003	0.006	1.154	76
+27°	0.050	−0.002	0.008	0.981	61
+36°	0.050	−0.003	0.007	1.058	76
+45°	0.060	0.002	0.011	1.072	34
+55°	0.050	−0.007	0.012	0.957	21
+65°	0.040	0.014	0.013	0.974	15
TXS	0.050	0.001	0.002	1.057	571

outliers were removed from the group, and the remaining 571 underwent an iterative process to bring the standard error of unit weight down to approximately unity in each declination strip by adjusting the excess error in each declination strip. The results of this process are summarized in Table 12.

In this table, the excess error is the rms value of error which was added in quadrature to make the standard deviation of unit weight approximately unity. The column labelled $\overline{\Delta r}$ is the resultant mean value of the log of the flux ratio; the column labelled $\sigma_{\overline{\Delta r}}$ is the standard deviation of the mean, and the column labelled σ_{uw} is the standard deviation of unit weight after the excess error has been added in.

The excess error must be regarded as particularly uncertain for the +55° and +65° catalog strips, due to the small number of calibrators, and in the case of the +65° catalog strip due to the fact that 8 of the 11 outliers removed in this analysis were from the edges of this strip.

The excess flux error in the residuals in this external comparison is probably due primarily to the rather poor state of flux density measurement at low frequencies. This is particularly true in the north, where a number of sources are dependent on measurements at 750 and 178 MHz dating back over 30 years. A second important contributing factor is the fact that an undetected mistaken structure model in the Survey can produce flux errors of 5%–10%. If one tenth of the sources are affected by such mistaken structure choices, an excess error of about 2.5% would be produced. A third contributing factor is the possibility of significant uncorrected diurnal gain changes, particularly in the +55° and +65° strips which have few calibrators. Finally, and probably least important, the flux density of many of the calibrators may be significantly time variable at the few percent level.

5. CONCLUSION

The Texas Survey lists 66841 sources over the 9.6 steradians between declination limits of $-35\overset{\circ}{.}5$ and $+71\overset{\circ}{.}5$ (B1950). Comparison with 408 MHz catalogs shows the central zone of the survey to have integral completeness ranging from 0.96 at a 408 MHz flux of 1 Jy down to 0.82 at 0.25 Jy; differential completeness ranges from 0.95 at 1 Jy to 0.50 at 0.25 Jy (see Table 5). Enumeration reliability is 99% at all flux levels (Table 6), while lobeshift incidence ranges from less than 1% for strong sources with no adverse flags to 50% for fainter sources which have lobeshift warning flags (Table 7).

The possibility of a lobeshift should be suspected if the Survey position differs from an external accurate position by an even number of lobeshift intervals in one coordinate, or by an odd number in both. The lobeshift interval is about 52″ for position lobeshifts; 26″ for structure lobeshifts. Thus, for example, a Survey source which is offset from an accurate position by 50″ in right ascension and by 50″ in declination is probably position lobeshifted (an odd number of position lobeshift intervals in both coordinates), while a source offset by 50″ in declination only is probably structure lobeshifted (an even number of structure lobeshift intervals in one coordinate). Alternate position and structure models may be calculated in either case (see Sec. *2.6.3*), but the listed flux density is not easily corrected, and in the case of structure lobeshifts, should be ignored.

Positions of survey sources are based on a large set of astrometric radio positions. Internal position errors are listed on each catalog line; for point sources they range from 2 arcsec in right ascension by 1 arcsec in declination for the fainter sources to 0.5 arcsec by 0.25 arcsec for the brighter sources. The total error is the quadratic sum of the listed internal error, plus a calibration error of about 0.2 arcsec (the actual value is taken from Table 9), and an excess error (probably due to centroid variation at different frequencies) of 0.4 arcsec. Any systematic error in the Survey position scale is less than 0.1 arcsec in each coordinate.

The listed flux densities are unbiased estimates of the total source flux density at 365 MHz provided the structure model is correct; the flux density of sources that are not point objects or compact-component doubles may be substantially underestimated and sources with component sizes greater than about 30″ may be missing from the catalog altogether. The flux densities are listed on a modified version of the flux scale developed by Wills (1973), which (having due regard for source spectra) is identical to the 408 MHz Wyllie scale used for the Molonglo 408 MHz catalogs. Internal flux errors are listed on each catalog line; for point sources the internal error is about 0.024 Jy plus 1.2% of flux density. The total error is the quadratic sum of the internal error listed on the catalog line, an additional percentage calibration error of about 1% (the actual value is taken from Table 9), plus an external excess error of about 5% (the actual value is taken from Table 12). Our knowledge of flux densities at low frequencies is inadequate at present to say what part of this external excess error is due to remaining Survey errors and what part is due to errors in the comparison source flux densities themselves.

Internal evidence for flux density variability which is independent of external flux error is noted in the Survey tables for 1336 of the 66841 sources; similar tests applied to a constant population would flag 668 sources as variable by chance. Thus, roughly half of the sources flagged as variable probably are in fact low-frequency variables.

The Texas Survey is the result of the combined effort of many people over the years—so many years that all (except the first author of this paper) have now moved on to other things. While each of the authors of this paper contributed to all areas of the project, each had a special area: JND—general direction; text of paper; FNB—design of source finder algorithms and much of the stacking code; FAB—operation of the telescope and validation of data; GWT—design of electronic and computer subsystems; CW—design of Survey software and Monte Carlo testing. We thank the following people who have made particularly significant contributions: Dr. Clinton C. Brooks and Dr. Gerard F. Moseley proved the viability of the space-frequency synthesis technique through construction and use of the prototype 245 MHz interferometer during 1966–1969; Dr. Moseley later coordinated the construction of the Texas Interferometer and UTRAO facilities in general. Many current Survey analysis routines originated in their work. The Texas Interferometer was constructed in 1969–1971; this was particularly assisted by the efforts of Frederick L. Beckner, James A. Isbell, and UTRAO Superintendant Dino R. Parenti and his staff. Pre-survey observations and analysis carried out in 1971–1973 form the basis of Survey procedures; important contributions to this work were made by former graduate students Drs. William D. Cotton, Frank D. Ghigo, and Frazer N. Owen. The Texas Interferometer in its final expanded and computer-controlled configuration came into operation in 1973, and the Survey (and resurvey for variability) occupied its time from then until it was shut down in 1989. The authors are grateful to those who have operated this instrument over the years, particularly to Grant C. Conant (UTRAO Superintendant) and to his predecessor Dino R. Parenti, and to the entire observatory staff, particularly to those who were with the project throughout its lifetime: Eliberto S. Franco, Pablo R. Rubio, and Samuel Whatley. The data processing group in Austin was particularly important in this information-intensive project. Diana B. Hearn, Kirk Webb, Jack Byrd, and their co-workers provided indispensable interest and assistance. Preliminary versions of the +18° and +36° strips from the Survey were available in the early 1980's; dissertation research carried out with these strips by Dr. David B. Garrett and Dr. Elizabeth P. Bozyan provided material assistance in validating the Survey. Our colleagues in the radio group, Drs. Paul D. Hemenway, Beverley J. Wills, and Derek Wills, have contributed broad-ranging advice and very particular assistance in areas too numerous to mention. The Texas Survey and operation of UTRAO have been supported by grants from the National Science Foundation (AST-81-01205 and its predecessors), the National Geographic Society, by the State of Texas, and by the organized research program of the University of Texas at Austin.

We dedicate this work to the memory of Harlan J. Smith, whose enthusiasm, support and inspiration were present at the beginning and remained unflagging throughout the long and difficult process, and whose presence at the end, though not physical, is nonetheless vivid.

APPENDIX A. FORMAT OF THE CATALOG TABLES

The catalog lines are in fixed column format, with 133 columns per line. The following five sample lines were selected from the catalog strips −12° (Table 3b), −01° (Table 3c), and +18° (Table 3e) to illustrate the most important features of the line format.

Each line has six major fields: the name field (columns 2–11), the code field (13–17), the position field (20–58), the flux field (60–91), the structure field (94–118) and the comments field (120–133); columns not within these fields are always blank.

A.1 The Name Field

The Texas Survey source name follows the B1950 convention: the name is constructed from the hours and minutes of right ascension, the sign of declination, and truncated tenths of degrees of declination. In case of duplicate names, the earlier source is assigned a suffix A, and the later a suffix B (see 0305−131A and 0305−131B in the sample list above). There was no need in the Texas Survey to assign C and later letters. The name (*tsnm*) thus has nine characters, and is in columns 3–11.

It should be noted that the names were assigned at the penultimate stage of data processing; slight changes in the position system, or change in the lobe finally adopted, has caused a few source names to be different from what would be constructed with the final position listed. This difference has been allowed to remain—this field is a name, not a position. It is recommended that external references to Survey sources have the prefix TXS before the listed name.

The catalog line quantities are all subject to the listed structure model, which was chosen by fitting a sequence of models of increasing complexity and choosing the best, with due regard for the increased number of parameters fit. Sometimes one or more simpler models produced an acceptable (if less "good") fit, and catalog lines for those models are included in Table 4. In such cases, the alternate model flag (*aflg*) in column 2 is set to an asterix, otherwise to a blank (see 0000+178 in the sample list above).

A.2 The Code Field

The code field contains five single-character flags which provide coded information on the quality of the fit, on the environment near the source, on the contrast perceived (or lacking) among the lobeshift choices considered by the lobe choice routine, and some summary characteristics of the chosen structure model.

Column 13 contains the value of *xpvrflg*, which is set to blank if the fringe visibility of the adopted structure model is within the first minimum on all three subbeams. Such a model is in the principle value region of our structure-fitting algorithm (the "PVR"—see Fig. 4). If the fringe visibility of the adopted structure model is near or beyond the first minimum in one or more subbeams, *xpvrflg* is set to the number of such subbeams (and thus may be 1, 2, or 3). Such models are XPVR models, and although they are often perfectly accurate, they are more subject to structure lobeshift than are the PVR models.

Column 14 contains the model flag (*mflg*). Parameters on the catalog line are calculated from 32 independent interferometer baselines, subject to the model listed, which was itself chosen to minimize residuals. If the residuals to the fit

```
.........1.........2.........3.........4.........5.........6.........7
1234567890123456789012345678901234567890123456789012345678901234567890
 *0000+178  2+++    0  0 34.397  .200    17 52 46.08  2.87    1.567  .
   0117+038  2+WW2   1 17 50.393  .241     3 52 19.36  3.59     .645  .
   0140-059   +++    1 40  8.073  .048    -5 59  6.84   .37     .870  .
   0305-131A 1+CC    3  5   .843  .053  -13  9 49.04   .38    2.201  .
   0305-131B  NXW    3  5 44.610  .212  -13 10 52.71  1.97     .513  .

.........8.........9........10........11........12........13........14
1234567890123456789012345678901234567890123456789012345678901234567890
035    -.3 .4    .7     63( 2) AD30(11)   36( 2) *       A 181
078    1.0        1.7X    38( 3)    D      -44( 5)   (+1,+1) D011
026    -.1 .5  10.1 *              P                     011
077    -.8 .4    .5X    57( 1) AD17( 2)  -66( 1)   (-1,+1)  121
073    -.7        .8X              P                     121
```

are consistent with the system errors, including both noise- and flux-dependent terms, *mflg* is assigned the value "+." For cases where the residuals are inconsistent with expected errors, *mflg* is assigned the value "C" (for "Caution"—marginal inconsistency), or "W" (for "Warning"—serious inconsistency). When the residuals are such that the model is clearly incorrect, *mflg* is set to "N" (for "No Model"), although the least bad model is used for producing the catalog line. It should be noted that many sources with *mflg*=N are in fact well-modeled, based on comparison to other work. In such cases the large residuals are often the result of near-by sources or of interference which happened to increase the rms residuals greatly while affecting the mean quantities on the catalog line by much smaller amounts. But of course, many "N" models are truly bad, and a few are attached to catalog lines which don't represent sources at all, but which are spurious responses.

The environment flag (*eflg*) in column 15 is set to "+" if the sky surrounding the source (as represented in the Survey itself) contains no other source which will contribute significantly to the fringe amplitudes at the catalog line source position. The contributions of other sources are calculated, and if their flux at the catalog line position is sufficient to contribute significantly to the residuals in one or more subbeams, *eflg* is set to "C," or to "W" if the contribution of the other source is expected to dominate the residuals. Occasionally, the interfering sources have a higher calculated flux density at the catalog line position that the catalog source itself, in which case *eflg* is set to "X." Some sources with *eflg*=X survive to the final Texas Survey listing, when other tests suggest the source is real. The environment flux calculation is conservative, and for example does not reflect the depth of envelope nulls that may lie in the direction of the potentially interfering source.

Column 16 has the lobeshift flag (*lflg*). Each tentative catalog line model is used to reduce the data on a grid of possible lobeshifted positions, and the best-fitting position is chosen. In many cases, this position is the only decent fit to the data, in which case *lflg* is set to "+." If another lobe position is possible, *lflg* is set to "C," and if it produces only a slightly worse fit to the data than the most probable position, *lflg* is set to "W." In the event that the second most likely position is the only remaining lobe position that is at all likely, its offset is given in columns 122–128 (see below).

As a complement to the structure information carried in *xpvrflg* in column 13, *lvflg* (low visibility flag) in column 17 is set to blank, 1 or 2 to indicate the number of subbeams on which the catalog line model has fringe visibilities less than 0.2. (It is impossible for all three subbeams of those models attempted to have visibilities less than 0.2). This information was used by Survey editing algorithms, and remains on the catalog line as an indicator of sources that are fit by models with essentially no flux on one or two subbeams, and which therefore may still be questionable.

Although the code field proper contains only the five flags just described, there are a number of other quality or comment flags in other fields (such as *aflg* in the name field). They will be described with their associated fields.

A.3 The Position Field

The B1950 position of the centroid of the listed structure model, together with its error, is listed in the position field. Beginning in column 20, the right ascension and its error is contained in four variables: *irh*, *irm*, *rs*, *sigra* in format $i2,x,i2,x,f6.3,x,f5.3$. Three blanks in columns 38–40 separate the right ascension subfield from the declination subfield, which begins in column 41, and has four variables: *idds*, *idm*, *ds*, *sigdec* (in format $a3,x,i2,x,f5.2,x,f5.2$), ending in column 58. Care should be taken in reading and decoding *idds*, the sign and degrees of declination, since many computers read a -0 as 0, thereby losing the sign information. The quoted errors *sigra* and *sigdec* are standard deviations of the fitted positions, based on the observed residuals to the fitted model, or are based on propagated noise, whichever is larger. They are thus purely internal errors, and do not reflect the error in adjustment of the survey position system to the position calibrators (typically 0.2 arcsec), nor do they include estimates of other types of excess error, such as residual systematic error or the centroid variance found when comparing to catalogs made at other frequencies. These matters are more fully discussed in Sec. *4.3*.

A.4 The Flux Field

The flux field begins in column 60 with the flux density subfield, which contains two flags and two variables: *sflg*, *flux*, *sigf*, *snflg* (format $a1,x,f6.3,x,f5.3,x,a1$), ending in column 75. The low flux flag *sflg* was incorporated as a convenience in the internal manipulation of the Survey, and is set to "X" if the source flux density is less than 0.15 Jy (925 sources), and is set to blank otherwise (65916 sources). The total 365 MHz flux density in Jy of the source given the listed model is *flux*. A fitted spectral slope over the operating frequency range 335–380 MHz has been removed and the error *sigf* (in Jy) is the standard deviation of *flux* given the observed residuals, or the propagated noise, whichever is greater. As was the case with position errors, *sigf* is a purely internal error.

Note that the value of *flux* will be a serious overestimate if a large D or AD model is erroneously used for a point source, and will be a serious underestimate if the reverse is true. The signal-to-noise ratio flag *snflg* in column 75 was incorporated as a convenience in internal manipulation and testing of the Survey. *snflg* was set to "X" if $s/n<4$ (and the source was not retained in the final catalog); to "Y" if $4\leqslant s/n<5$ (2475 sources); to "Z" if $5\leqslant s/n<7$ (8480 sources), and to blank if $s/n\geqslant 7$ (55886 sources).

Following a blank in column 76, the spectral index subfield begins in column 77, and contains two variables: *gam* and *siggam* (format $f4.1,x,f2.1$), ending in column 83. Since the Texas Survey is carried out on at least two of the three frequencies 335, 365, and 380 MHz, estimation of the flux density at the standard frequency of 365 MHz involves fitting a spectral index *gam* to the data; *siggam* is the standard deviation of the fit based on observed residuals. The source spectral index is defined in the sense: $\log(flux)\propto gam \times\log(f)$. Naturally, the error in the spectral index is high given the small frequency range involved, but a useful indication of the spectrum is afforded in many cases. When the error *siggam* is greater than 0.9, *siggam* (columns 82–83) is left blank, and the value of *gam* if present should be treated with suspicion. A number of sources have blanks in both the *gam* and *siggam* fields; they represent instances where *gam* could not be determined or in the case of lines from TS6 (see definition of *strp* below) are sources whose *siggam* is greater than 0.8. For the Survey as a whole, useful spectral indications are given for 24558 of 66841 sources. Columns 84 and 85 are always blank as a divider before the next subfield.

The variability subfield begins in column 86 and contains one variable and two flags: *var*, *vflg*, and *vstar* (format $f4.1,a1,a1$), ending in column 91. *var* is the sum of the squared standardized residuals to the flux density of the modeled source on each of the four observing cycles. It has a χ-squared distribution with 2 degrees of freedom (2 were lost by fitting flux and spectrum); values of *var* greater than 5.99 would be expected for 5% of nonvariable sources; values greater than 9.21 would be expected for 1%, and values greater than 13.82 would be expected for 0.1%. Since a spectral slope is removed, a variable source may also show up by virtue of having a very odd spectral index. Taking both factors into account, *vstar* is set to "*" if *var* is greater than 9.21 (the 1% level), or if *gam* is less than $-1.5-2\times siggam$ or greater than $0.5+2\times siggam$; otherwise *vstar* is left blank. If the value of *var* is suspect (*mflg* not "+," or fewer than six baselines present in any one observing cycle, or the normalized χ-squared residual for any one observing cycle was greater than twice the number of baselines present), *vflg* in column 90 is set to "X" rather than to blank, and a variability indication in *vstar* should be treated with due caution. For the 343 source lines that come from TS6 (see definition of *strp* below), the entire variability subfield is left blank rather than setting *vflg* to "X." For the Survey as a whole, 49144 sources have variability parameters which are not suspect; 904 of these are marked as possibly variable (at the 1% level), and 17697 sources have suspect variability parameters, and 432 of these are marked as possibly variable.

A.5 The Structure Field

The structure field format varies with the structure model adopted. If the point model is adopted, column 105 is set to "P" and the rest of the structure field (94–118) is blank.

The format for the symmetric double model has column 105 set to "D," and four variables are included: the double component separation *isep* and its error *iseperr* (both in integer arcsec), and the position angle *ixi* (increasing north through east) and its error *ixierr* (both in degrees). The format is $i3,x,i2,11x,i4,x,i2$; the columns skipped over contain blanks or formatting constants such as "("and")"—see the sample listing for 0117+038.

The format for the asymmetric double model is implied if column 105 is neither "P" nor "D"; it includes the separation and orientation quantities as in the "D" model and two more variables as well: the asymmetry parameter q (listed as $iqq=q\times100$) and its error *qerr* (listed as $iqerr=qerr\times100$).

These are appended to the ''AD'' code, and appear between the separation and orientation quantities; see the sample listing for 000+178 and 0305−131A. Thus, in the AD format, the variables are read in the order *isep*, *iseperr*, *iqq*, *iqerr*, *ixi*, *ixierr* in the format *i*3,*x*,*i*2,4*x*,*i*2,*x*,*i*2,2*x*,*i*4,*x*,*i*2.

A.6 The Comments Field

Columns 120–133 constitute the comments field, and contain four flags and three variables. The Survey was reduced in ten declination strips, in which regions near the edges overlap with adjacent strips, and each declination strip was reduced in right ascension segments, with intersegment boundaries also having overlap. Only one version of such overlap sources was chosen for inclusion in the catalog, and *raoflg* in column 120 is set to ''*'' to denote the chosen catalog line, and to ''$'' to designate the other. The TXS tables thus only have blank or asterisk in column 120. The declination overlap flag *decoflg* in column 121 is similarly encoded. Sources which are in overlap zones are designated by *raoz* (column 129; *raoz*=A–E, or blank if not in *ra* overlap zone) and by *decoz* (column 130; *decoz*=A–K, or blank if not in *dec* overlap zone).

In some cases the lobe selection routines find that the second most likely lobe choice, although inferior to the most probable choice, is nonetheless far better than any of the other possibilities. The offsets *ka*2 (i.e., the k_α) and $kd2(=k_\delta)$ of the second most likely lobe are in columns 123,124 and 126,127; see the sample lines for sources 0117+138 and 0305−131A.

The variable *strp*, in a3 format in columns 131–133, describes the observation strip and segment from which the catalog line was obtained. For example, looking at the sample line for 0000+178, *strp*=181 means the catalog line came from the +18° observation strip, *ra* segment 1 (although since it is in *ra* overlap zone A, its catalog line could have come from *ra* segment 5). Furthermore, some sources in the +18° strip came from an entirely different reduction from the rest of the Survey (although using the same observational data and the same position and flux system); these are designated *strp*=TS6, for Texas Survey, Version 6 (the main Survey reduction is Version 7). There are slight differences in format in these lines, as explained under the discussion of the spectrum and variability subfields above.

APPENDIX B. FORMAT OF THE TABLES OF SIMPLER MODELS

The tables of simpler models (Tables 4a–4j) have the same format as the catalog tables, but with certain information omitted. The variability subfield (columns 86–91) is blank, as are the errors in the structure parameters and columns 120–128 of the comments field.

Furthermore, the sources are not in strict right ascension order, but are rather in the order of appearance of their corresponding catalog entry in the catalog tables. Note also that a number of sources have more than one simpler model listed.

REFERENCES

Baars, J. W. M., Genzel, R., Pauliny-Toth, I. I. K., & Witzel, A. 1977, A&A, 61, 99

Bash, F. N., & Douglas, J. N. 1974, A&AS, 15, 457

Bash, F. N., Cotton, W. C., & Douglas, J. N. 1974, AJ, 79, 1341

Colla, G., *et al.* 1970, A&AS, 1, 281 (B2.1)

Colla, G., *et al.* 1972, A&AS, 7, 1 (B2.2)

Colla, G., *et al.* 1973, A&AS, 11, 291 (B2.3)

Cotton, W. C., Owen, F. N., & Ghigo, F. D. 1975, AJ, 89, 353

Davies, I. M., Little, A. G., & Mills, B. Y. 1973, Australian J. Phys. Astrophys. Suppl., No. 28. (MC1)

Douglas, J. N. 1961, Northeast Electronics Research and Engineering Meeting (NEREM) Record 1961, p. 88

Douglas, J. N., & Brooks, C. C. 1962, AJ, 67, 575

Douglas, J. N. 1965, Northeast Electronics Research and Engineering Meeting (NEREM) Record 1965, p. 224

Douglas, J. N., Bash, F. N., Ghigo, F. D., Moseley, G. F., & Torrence, G. W. 1973, AJ, 78, 1

Douglas, J. N., & Bash, F. N. 1977, in Radio Astronomy and Cosmology, edited by D. L. Jauncey (Reidel, Boston), p. 15

Douglas, J. N., Bash, F. N., Torrence, G. W., & Wolfe, C. 1980, Publ. Dept. Astron. Univ. Texas, No. 17, October, 1980

Douglas, J. N., & Davis, M. M. 1981 (private communication)

Fanti, C., Fanti, R., Ficarra, A., & Padrielli, L. 1974, A&AS, 18, 147 (B2.4)

Ghigo, F. D., & Owen, F. N. 1973, AJ, 78, 848

Goldstein, S. J. 1959, ApJ, 130, 393

Gregory, P. C., & Condon, J. J. 1991, ApJS, 75, 1011

Large, M. I., Mills, B. Y., Little, A. G., Crawford, D. F., & Sutton, J. M. 1981, MNRAS, 194, 693 (MRC)

Moseley, G. F., Brooks, C. C., & Douglas, J. N. 1970, AJ, 75, 1015

Rees, N. 1990, MNRAS, 243, 637

Robertson, J. G. 1973, Australian J. Phys., 26, 403

Scott, P. F., & Shakeshaft, J. R. 1971, MNRAS, 155, 19P

Sharp, J. R., & Bash, F. N. 1975, AJ, 80, 335

Sutton, J. M., Davies, I. M., Little, A. G., & Murdoch, H. S. 1974, Australian J. Phys. Astrophys. Suppl., No. 33 (MC2, MC3)

Swenson, G. W., & Mathur, N. C. 1969, Radio Sci., 4, 69

Vitkevitch, V. V. 1953, Proc. Acad. Sci. USSR, 91, 1301

White, G. L. 1983, Ph.D. thesis, University of Sydney

Wills, B. J. 1973, ApJ, 180, 335

Wyllie, D. V. 1969a, MNRAS, 142, 229

Wyllie, D. V. 1969b, PASAu, 1, 234